Using Geothermal Energy To Mix the Ocean

John Reid and Peter Nielsen

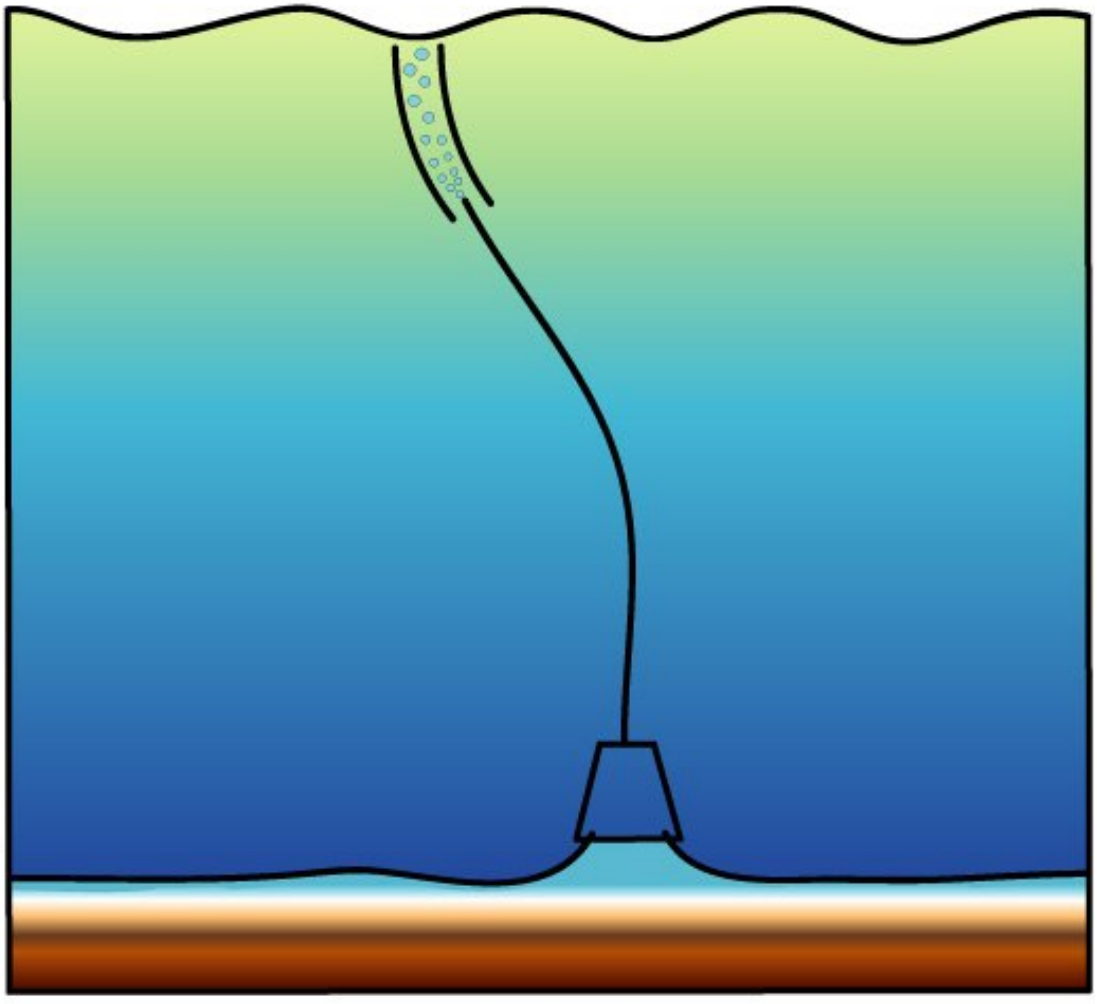

Released 19 December 2007 by:

Ecofluidics Pty Ltd
12 View Street
Sandy Bay
Tasmania 7005

ACN 091 770 339

Authors:

John Reid
PO Box 279
Cygnet
Tasmania 7112
jreid@olrig.com.au

Peter Nielsen
12 View Street
Sandy Bay
Tasmania 7005
uusi@gotalk.net.au

Cover Design: Richard Stanley

Summary

- There are environmental advantages in mixing the upper layers of the ocean by bringing deep nutrients into the light where photosynthesis by phytoplankton, the base of a very important food chain, can occur.

- These advantages include augmenting the volume and diversity of ocean fish stocks and sequestration of atmospheric CO_2 in the deep ocean.

- The energy to carry out oceanic mixing is available in the form of superheated water from hydrothermal vents (HTVs) on the ocean floor.

- A heat engine has been devised in the form of a large scale bubble pump which converts HTV superheated water into the mechanical energy needed to bring nutrient-rich water to the surface.

- The cost of construction and deployment of such bubble pumps can be justified economically in terms of the commercial fish stocks created and by the carbon credits traded.

- There are both sufficient nutrients and sufficient energy available to allow such schemes to be developed for decades to come, even to undo recent increase in atmospheric CO_2.

Contents

1 Overview

Ocean covers seventy percent of the earth's surface and ninety percent of the ocean surface is a desert. The blue water seen between the clouds in satellite images is desert. Productive waters are always green in colour.

The reason for the almost complete absence of living organisms is a lack of nutrient. Phytoplankton, the "grass" of the sea at the bottom of the food chain, requires nitrate, phosphate, iron and silicate in order to thrive and these are absent from much of the ocean's surface.

Unlike deserts on land where the missing ingredient is usually water which may lie hundreds of kilometres away, the nutrients needed by the ocean are only hundreds of metres distant; hundreds of metres vertically downwards at depths to which the sun's rays cannot penetrate.

All that is needed for the desert ocean to bloom is to mix these nutrient-rich deeper waters into the sunlit surface layer so that photosynthesis can take place. Mixing nutrients into the desert-like parts of the ocean in this way will have two desirable effects, viz,:

- it will bring a new marine ecosystem into existence comprising phytoplankton, zooplankton, small fish and ultimately bigger commercial fish, and

- it will bring about a net loss of carbon dioxide from the atmosphere.

However it requires energy to mix the ocean. Below about 50m or so beneath the surface the ocean is highly stratified. The deeper water is colder, saltier and denser than the surface water and it requires energy to lift it up to the surface against the action of gravity.

Where then is energy to be found in the deep ocean to bring about this mixing process? Wind and wave energy are candidates. Ocean thermal energy conversion (OTEC) is also a candidate energy source. In order to be useful the mixing needs to be done on a very large scale. Flows comparable with major rivers need to be generated. It is doubtful if the energy sources mentioned above would be sufficiently powerful for the task.

There is another energy source in the ocean. Running along the middle of the major oceans are mid-oceanic ridges (MORs), ~60,000 km of them. These are fissured mountain ranges generated by the upwelling of magma along the cracks between the continental plates. They are places where the plates of the earth's crust are pulling apart from one another and hot subterranean magma (i.e. lava) comes very close to the surface of the crust due to the “pulling apart”.

Indeed the magma come so close to the surface through this porous crust along MORs that it makes contact with ocean water which becomes very hot and wells up through the ocean floor in the form of hydrothermal vents (HTVs).

These vents, which were first seen in 1977 are also called "black smokers" because of their appearance. Their dark colour is due to black metal sulphides which have dissolved out of the hot rock, and which precipitate out as the vent water cools.

As possible energy sources these are very good candidates indeed. Each vent puts out 5 to 10 MW (Megawatts) of power (in the form of heat) and there are many of them. Of 60,000 km of mid oceanic ridges, only ten percent had been explored at the time of writing. Wherever the ridges have been explored, hydrothermal vents have been found. According to Dr Robert Reves-Sohn of the Woods Hole Oceanographic Institute, the thermal power of black smoker flow from a single vent field, the TAG field on the Mid-Atlantic Ridge is at least 1 GW (Personal Communication and Wichers et al 2005). The total power from all such fields could well be in excess of 10 terawatts.(i.e. "from a single vent field")

Unfortunately this HTV energy only comes in the form of heat. It will require mechanical energy to mix the ocean. As we recall from high school physics - it is easy to convert mechanical energy to heat (via friction) but it is much harder to convert heat to mechanical energy because of the Second Law of Thermodynamics.

Nevertheless it can be done. Machines which do this are called heat engines. The steam turbine which generates electricity is an examples of such a heat engine. However it gets better than that.

The hot water from the HTVs is not just any old hot water, it is superheated hot water. Its temperature is 360^{o}C, well above the boiling point at the surface of the ocean and comparable with the temperatures at which steam turbines run. The only reason this water does not boil at the HTVs is because, at that depth, typically, 2500m, the water is under huge pressure - 250 atmospheres. The higher the pressure the greater the temperature needed to make water boil.

So the vent water does not normally boil. It rises up a couple of hundred metres then spreads out horizontally like smoke from a chimney on a frosty night.

Now suppose we channel this superheated water towards to the surface in an insulated pipe. As it gets closer to the surface and the pressure decreases it will start to boil. There is a change of state from water to steam. All that is needed to make a heat engine work is such a change of state.

This change of state generates three things - energy, momentum and buoyancy. It turns out that using the buoyancy is the best way to bring about ocean mixing. We use the buoyancy of the newly generated steam**,** in the form of a steam and water foam passed to a second pipe as a very large bubble pump. Hitherto

bubble pumps have only been made on a very small scale**,** used in things like gas driven refrigerators.

Such a hydrothermal bubble pump or HTBP is illustrated in Figure 1.1. For the purposes of illustration the horizontal scale in Figure 1.1 is exaggerated. The vertical extent of the diagram is 2500m but the fat pipe at the top is only about 10m in diameter or 1/40th of its length.

It turns out that bubble pumps will work on a large scale and can be used to mix the surface layers of the ocean.

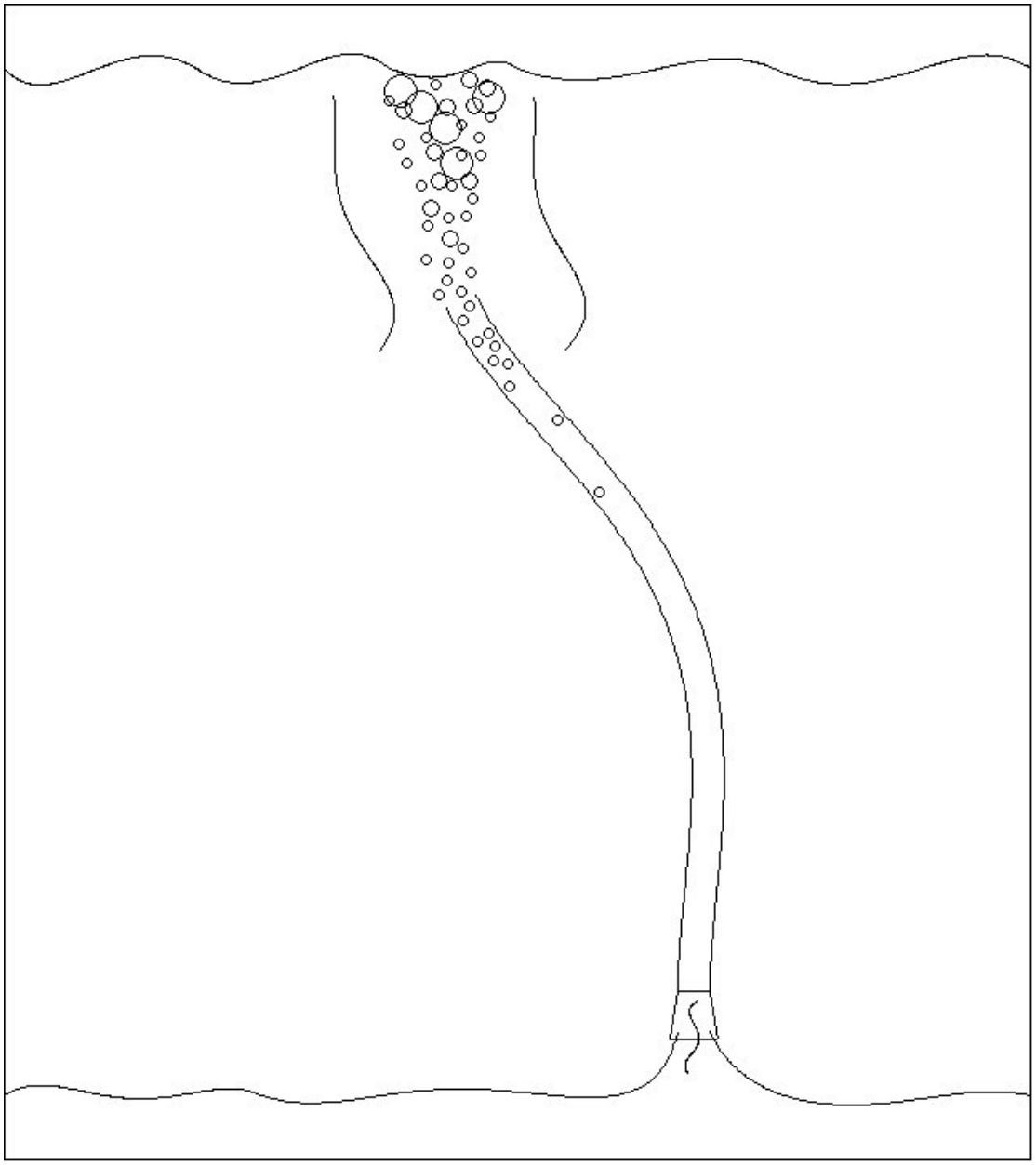

Figure 1.1

2 The Thin Pipe Model

Introduction

The idea of using the energy of hydrothermal vents to mix nutrient into the near surface ocean has been through a number of iterations since a provisional patent application was first filed in March 2007. It is therefore important that these ideas be set out and distinguished from the most recent embodiment so that there is no misunderstanding about which version is under discussion.

The Fat Pipe Embodiment

The first of these was the original "Fat Pipe" idea whereby the vent plume is confined in a large pipe (say 100m in diameter) made from a light, non-heat-resistant material such as polystyrene. The pipe allows mixing with seawater surrounding the vent in a ratio of 30:1 to cool the plume down to say 10 deg C. The warm water mixture is then carried up the pipe by convection bringing nutrients with it. The purpose of the pipe is to inhibit entrainment of further cold water thus preventing the plume from cooling down to the point where it would spread horizontally at depth in the manner of natural plumes.

This idea is flawed in two ways. On the one hand bottom waters are not a rich source of nutrients and convection is an inefficient method of pumping fluids.

The Thin Pipe Embodiment

The next idea was to bring about a phase change by raising the vent water in a heat-resistant thermally insulated pipe to a depth at which the hydrostatic pressure is sufficiently low to bring about boiling . Boiling greatly amplifies the volume flux for a given mass flux and high velocities can be generated. The top end of the pipe is fitted with an appropriately shaped nozzle, similar to a jet engine nozzle, which maximizes the momentum delivered to the water column. The resulting jet adds turbulent kinetic energy to the surrounding water which deepens the mixed layer by creating a toroidal eddy.

However, Newton's Third Law gives rise to a reaction which will cause the pipe to buck like an unrestrained fire-hose unless vanes and/or a floatation collar are used to inhibit this motion.

This idea too is flawed. The exit velocity from the nozzle cannot exceed the speed of sound in the medium being expelled. The medium in question is a hot sea-foam comprising 30 percent steam by mass. The velocity of sound in such a water-steam mixture will be lower than in either water or steam alone. According to some writers it could be as low 20 m/s.

A further difficulty is that the sea-foam generated in this way will mix rapidly with surrounding cold water and will condense back to water as soon as it emerges from the nozzle so that any buoyancy effects are immediately lost.

The Hybrid Embodiment

This last consideration lead to the realization that it is not desirable to mix the sea foam with the surrounding water. Generating a high velocity sea foam jet is not desirable, even if it were possible because a high degree of entrainment of surrounding cold water would result in the rapid annihilation of the bubble stream.

One way of minimizing contact between the sea foam and the surrounding water is to release the sea-foam at low velocities and high volume flux rates. This idea lead directly to the third embodiment, which is a hybrid embodiment involving both a fat pipe and a thin pipe.

An insulated thin pipe brings vent effluent from the ocean floor to well above the level at which it boils, so generating foam within the pipe. The foam is injected into the fat pipe. The foam bubbles reduce the mean density and total mass of fluid within the fat pipe which is open at both ends. As a result there will be a net body force on the fluid within the fat pipe causing it to move upwards. This continued vertical movement of water results in cold water entering the bottom of the fat pipe to be delivered to the region surrounding the top of the fat pipe. In practice the bottom of the fat pipe will be placed at a level where nutrient concentration is high and the top of the fat pipe will be in the mixed layer or euphotic zone where nutrient levels are low but where photosynthesis can occur.

This embodiment does not suffer from the flaws inherent in the first two embodiments described above. It utilizes buoyancy alone rather than momentum or turbulent kinetic energy to bring about ocean mixing. Velocities are lower so that turbulence and the mixing of hot foam and cold sea water are minimized as are Newton's Third Law effects.

Numerical Modeling

Now that a mechanism has been clearly defined it is possible to model it. Various levels of detail and sophistication are possible depending on the simplifying assumptions that are made. At this stage of development a simple energy budget model constitutes an essential first step and that is all that will be dealt with here. This energy budget model will provide a useful basis for a more thorough hydraulic model which is developed below.

Hydrothermal Vent Assumptions

The starting point for the model is the mass flux and temperature of the hydrothermal vent (HV) effluent which is the energy source. Much of the literature on HVs deals with their biology and good physical data is hard to find.

Typically vents are quoted as producing 5 to 10 MW of power. Effluent temperatures are better known and a figure of 360° C is widely quoted. The significance of this temperature is that it is the reaction temperature at which silicates are formed and dissolved when sea water contacts hot subterranean magma. Assuming the temperature of benthic sea water is 4 deg C and that this has been warmed through $\Delta T = 356°$ C the specific heat of water can be used to derive a mass flux from the quoted power. Thus

$$mass\ flux = vent\ power\ /\ (\Delta T * specific\ heat)$$

It is assumed that the entire output from the vent is captured by the thin pipe at the effluent temperature of 360° C.

Thin Pipe Assumptions

Flow in the thin pipe will be high Reynolds number (turbulent) flow. For a given the diameter, length and roughness of the pipe and the pressure head difference, the upward velocity can be determined by the usual methods of hydraulics. This velocity is a strong function of pipe diameter. Here this calculation is skipped and it is assumed that the pipe diameter has been fixed at a value which yields a mass flux up the pipe that is numerically equal to the HV mass flux derived above.

One aspect of thin pipe performance which cannot be ignored however is the loss of heat through the walls of the thin pipe. A temperature difference of hundreds of degrees is involved so that the pipe must be well insulated. The coefficient of thermal conductivity, k, of the pipe walls is the most crucial design parameter for reasons which will shortly become apparent.

Because ocean stratification is a vital aspect of the operating environment a realistic profile of salinity and temperature taken from WOCE Section P18 at latitude 45° S and longitude 155° E. The profile is shown in Table 2.1. The pressure and density values in Table 2.1 were computed using an algorithm published by McDougall et al (2002). This profile was used to determine values of ambient quantities in all subsequent calculations.

The temperatures at which water boils at a given pressure, the saturation temperature, T_{sat}, was derived using algorithms published by the International Association for the Properties of Water and Steam (IAPWS). They are valid for temperatures between 273.15 K and 863.15 K. Although these algorithms only apply to fresh water they were deemed good enough for present purposes because corresponding algorithms for seawater could not be found.

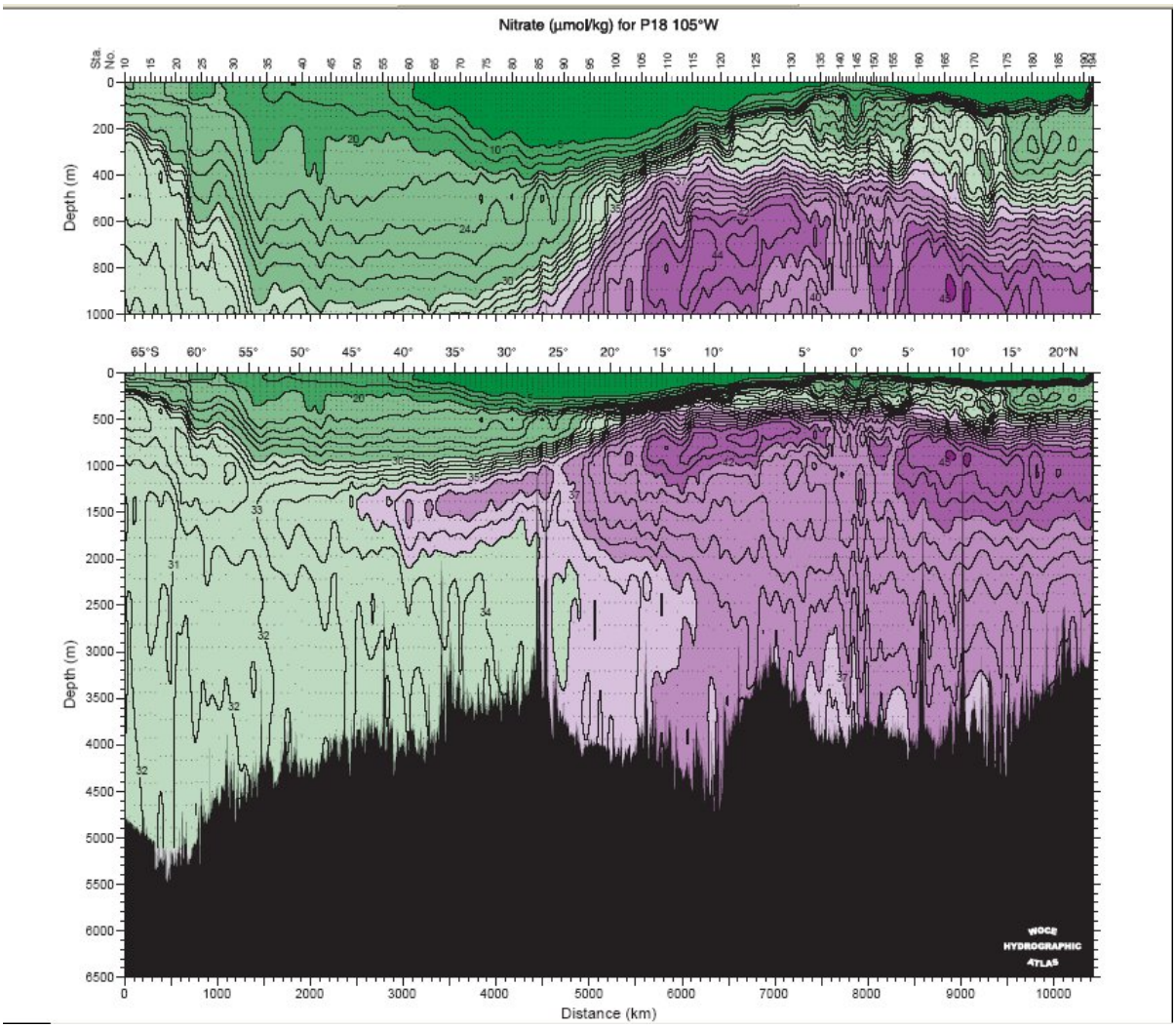

WOCE P11 45 deg S 155 deg E

j	Depth	Salinity	Temp	Pressure	Density
1	0	34.80	13.80	10.00	1026.12
2	100	35.10	11.90	110.66	1026.88
3	200	34.85	10.30	211.40	1027.54
4	300	34.75	9.60	312.20	1028.11
5	400	34.66	9.00	413.06	1028.64
6	500	34.60	8.50	513.97	1029.15
7	600	34.56	8.10	614.93	1029.65
8	700	34.50	7.40	715.94	1030.16
9	800	34.47	6.70	816.99	1030.68
10	900	34.42	5.80	918.11	1031.22
11	1000	34.40	5.00	1019.27	1031.77
12	1500	34.52	2.80	1525.35	1034.30
13	2000	34.68	2.20	2032.68	1036.81
14	2500	34.73	1.80	2541.23	1039.24

Table 2.1

Conductive Cooling of the Thin Pipe Fluid

The cooling of the vent effluent as it journeyed up the thin pipe was determined as follows. A test volume was considered which traveled up the pipe with velocity, w, determine by dividing the volume flux by the pipe area. The heat lost in time dt from the test volume is given by

$$dQ = kA\Delta T dt \; / \; l$$

where k is the Coefficient of Thermal Conductivity, A is the area of fluid in contact with the walls of the pipe, l is the wall thickness of the pipe and ΔT is the temperature difference between the exterior and interior of the pipe. This difference can be expressed as

$$\Delta T = T_a - T$$

where T_a is the ambient temperature on the outside of the pipe.

The rate of cooling of the test volume is determined by

$$dQ = mc_l dT_c$$

where m is the mass of the test volume and c_l is the specific heat of water and dT_c is the incremental temperature increase due to the incremental heat gain dQ. In our case both dQ and dT_c will be negative because ΔT is negative.

Using the chain rule

$$dQ/dt = (dQ/\; dT_c).(\; dT_c \; /dt)$$

gives

$$dT_c \; /dt = k.A.\; \Delta T \; / \; m.\; c_l.l$$

Substituting using $m = \rho V$, $V = \pi D^2 h/4$ and $A = \pi D$ gives

$$dT_c/dt = 4k\Delta T \; / \; c_l \rho D l$$

where D is the diameter of the pipe and ρ is the density of the fluid in the pipe which is assumed to be entirely liquid for the purpose of this calculation. Finally using continuity

$$dT_c \; /dz = (1/\mathrm{v}).dT_c/dt$$

and the temperature, $T(z)$, can be found as a function of depth, z, by numerically integrating from the bottom of the pipe upwards using external temperature

values determined by interpolating between the depths values given in Table 2.1. The density, ρ, is determined substituting the previously computed value of T and the initial salinity and the ambient pressure into the McDougall et al algorithm for the equation.

The quantity

$$\tau = c_l \rho D l \ / 4k\Delta T$$

has the units of time and is the e-folding time for the temperature decay in a uniform ambient temperature, T_a.

The above described calculation is entirely hydrostatic and includes neither the Bernoulli Effect nor pipe friction in the calculation of pressure.

Vent Temperature =	360 degC
Vent Power =	10 MW
Vent Mass Flux =	6.671 kg/s
Vent Volume Flux =	0.007673 m3/s
Pipe Salinity =	34.730 psu
Pipe Diameter =	0.030 m
Coeff. of Thermal Cond. =	0.020 W/m.degC
Specific Heat =	4.19 kJ/kg.degC
Pipe Wall Thickness =	0.020 m
Pipe Velocity =	10.855 m/s

Table 2.2

Boiling

Table 2.2 lists values used in the calculations. Values for Coefficient of Thermal Conductivity and wall thickness were taken from a web brochure advertising WDS Flexible Pipe.

Figure 2.1 shows pipe temperature as a function of depth when the above parameters are used in the integration. Also shown in Figure 2.1 is the saturation characteristic for water and steam.

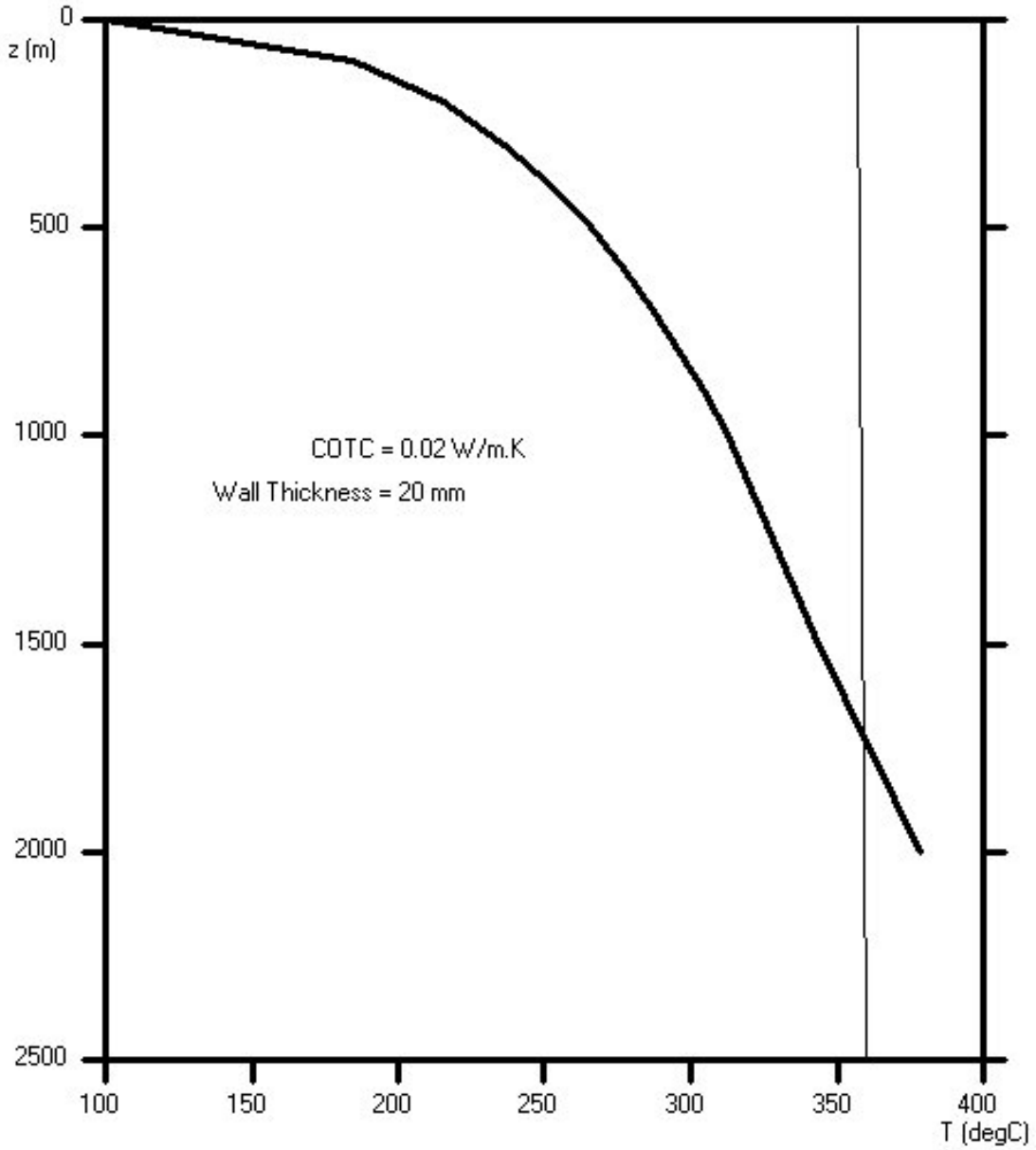

Figure 2.1. Decay of temperature with decreasing depth for the thin pipe when boiling is ignored (thin line). Also shown is the saturation characteristic for water and steam (thick line).

The intersection point of the two curves is at 1720m depth and 358.7° C. It is at this point in its upward journey that sea water will begin to boil. Once boiling occurs the temperature of the fluid will fall to a level at which boiling ceases. In this way the temperature of the pipe fluid follows the saturation curve giving rise to the more realistic temperature curve shown in Figure 2.2.

As a parcel of fluid ascends the pipe an increasing fraction of liquid-vapour mixture is converted to vapour by the heat it carries with it.
This vapour fraction depends on the latent heat of steam, L_v, and the specific heat capacity of the liquid-vapour mixture. The latter can be approximated by the specific heat capacity, c_l, of the liquid phase alone.

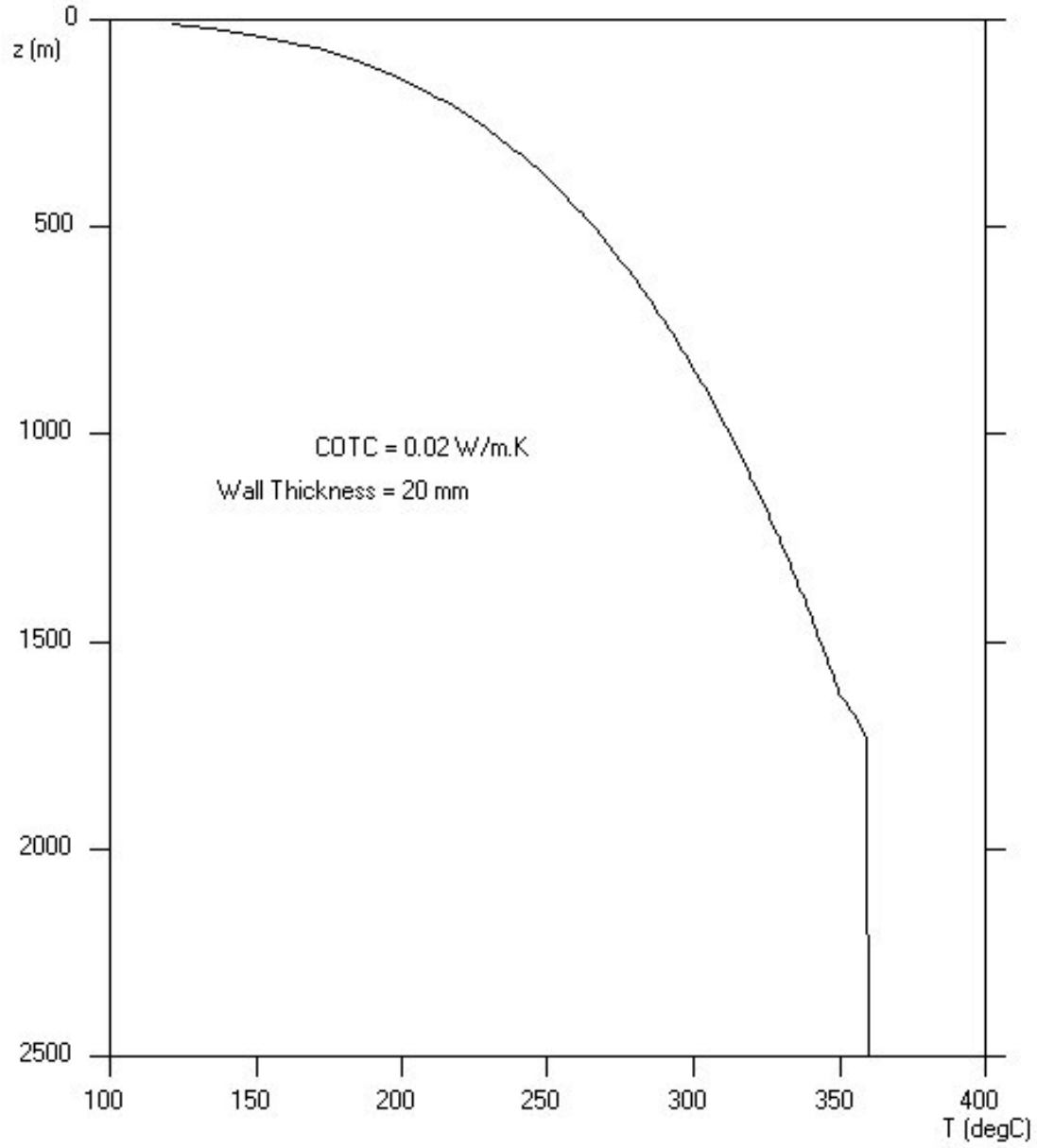

Figure 2.2. Decay of thin pipe temperature with decreasing depth when boiling is taken into account.

In the integration of temperature the parcel now experiences two temperature decrements, viz: one due to conductivity losses, dT_c, as before, and one due to latent heat loss, dT_L.

As before dT_c is given by

$$dT_c = (T_a - T)dt \; / \; \tau$$

while dT_L is given by

$$dT_L = T - T_{sat} \qquad if \; T > T_{sat}$$

$$dT_L = 0 \qquad if\ T \leq T_{sat}$$

The incremental increase in the vapour fraction of the parcel, dm_v is given by

$$dm_v = c_l m dT_L \ / \ L_v$$

where m is the total mass of the parcel and L_v is the latent heat of steam.

The new temperature of the parcel after time step, dt, is simply

$$T = T_{sat}$$

The new masses, volumes and densities of the parcel are given by

$$m_l = m_l - dm_v$$

$$m_v = m_v + dm_v$$

$$V_l = m_l \ / \ \rho_l$$

$$V_v = m_v \ / \ \rho_v$$

$$\rho = m \ / \ (V_l + V_v)$$

where the subscripts l and v refer to the liquid and vapour phases respectively, ρ_l is found from the equation of state for sea water as before and ρ_v is derived from the ideal gas equation. The quantity ρ is the density of the foam.

Sample output with depth step, dz, set to a coarse value of 100m for display reasons is shown in Table 2.4. Note the large (50 X) increase in volume of the fluid mass at 100m depth compared with its volume at 2500m depth. This large increase in volume is brought about by the change of state from liquid to gas. In Table 2.4 the column labeled "Fv" lists the fraction of the fluid which is vapour. At 100m depth 27.62% of the fluid is in the vapour phase. A bubble this hot sea-foam is injected into the fat pipe where its lower density causes water to be accelerated upwards.

jz	depth	Temp	Fv	Volume
25	100	184	0.2762	0.3572
24	200	215	0.2326	0.1712
23	300	236	0.2020	0.1074
22	400	252	0.1776	0.0757
21	500	266	0.1569	0.0570
20	600	277	0.1387	0.0447
19	700	288	0.1224	0.0361
18	800	297	0.1075	0.0299
17	900	305	0.0938	0.0251
16	1000	313	0.0811	0.0213
15	1100	320	0.0691	0.0184
14	1200	326	0.0579	0.0159
13	1300	332	0.0472	0.0139
12	1400	338	0.0371	0.0123
11	1500	344	0.0275	0.0109
10	1600	349	0.0183	0.0097
9	1700	357	0.0035	0.0081
8	1800	359	0.0000	0.0077
7	1900	359	0.0000	0.0077
6	2000	359	0.0000	0.0077
5	2100	359	0.0000	0.0077
4	2200	360	0.0000	0.0077
3	2300	360	0.0000	0.0077
2	2400	360	0.0000	0.0077
1	2500	360	0.0000	0.0077

Table 2.4

3 Theoretical Maximum Yield

Bubble Potential Energy Rate

Once the volume flux of sea foam into the fat pipe has been determined it becomes possible to work out how much cold deep water can be brought to the surface in a given time interval.

A stationary foam bubble located at a particular depth in the fat pipe has a particular potential energy associated with it. It is the work that would be done in taking the same bubble at the surface and pushing it downwards against buoyancy forces until it reaches the depth in question. For notational simplicity we will assume the bubble contains the mass of sea foam that would be delivered in one second from the thin pipe as computed above. The potential energy of this bubble is the bubble potential energy rate, BPER. It is the rate at which new potential energy is delivered to the fat pipe.

Specific Potential Energy

Similarly the potential energy required to move unit mass of deep cold water to the surface is the work done in lifting the mass from the initial depth against the force of gravity whilst taking buoyancy due to the surrounding fluid into account. Since we are dealing with unit mass we can call this the specific potential energy, SPE, of the cold deep water.

A Definition of Yield

The mass of cold water that can be brought to the surface from depth in one second, the yield, is the bubble potential energy rate divided by the specific potential energy of the cold deep water.

The calculation of both of these quantities is simply a matter of integrating the body forces over height while taking the change in buoyancy due to changes in volume into account.

For present purposes there are only two free parameters associated with the fat pipe, viz: the nozzle depth, ND, the depth at which the bubble is injected by the thin pipe, and the depth of the bottom of the fat pipe from which the cold nutrient rich water is drawn, termed here the reference depth, RD.

These quantities and their ratio, the yield, are listed in Table 3.1 for various runs of the numerical model for a selection of nozzle depths and reference depths.

Yields shown in Table 3.1 are of the order of ½ million to 1 million Kg/s for a 10 MW HV at 2500m depth.

RD (m)	ND (m)	BPER (J/s)	SPE (J/Kg)	Yield (Kg/s)
400	100	891285	1.191	748580
400	200	1148612	1.191	964707
400	300	1284023	1.191	1078437
400	400	1371079	1.191	1151554
500	100	891285	1.396	638497
500	200	1148612	1.396	822840
500	300	1284023	1.396	919845
500	400	1371079	1.396	982210
500	500	1432380	1.396	1026125
600	100	891285	1.609	553882
600	200	1148612	1.609	713796
600	300	1284023	1.609	797946
600	400	1371079	1.609	852046
600	500	1432380	1.609	890142
600	600	1477824	1.609	918383
700	100	891285	2.028	439485
700	200	1148612	2.028	566372
700	300	1284023	2.028	633141
700	400	1371079	2.028	676068
700	500	1432380	2.028	706295
700	600	1477824	2.028	728703
700	700	1512610	2.028	745856
800	100	891285	2.651	336260
800	200	1148612	2.651	433343
800	300	1284023	2.651	484430
800	400	1371079	2.651	517274
800	500	1432380	2.651	540402
800	600	1477824	2.651	557547
800	700	1512610	2.651	570671
800	800	1539794	2.651	580926

Table 3.1

A Cautionary Note

The calculated yields listed in Table 3.1 are maximum theoretical yields. They are the yields which would be obtained in the absence of pipe friction and heat losses and under the assumption that the various parcels of water move so slowly that kinetic energy considerations can be ignored. In practice none of these things are true. The hydrothermal bubble pump described here is a type of heat engine and will experience energy losses due to all of these effects. A more realistic figure is obtained in the next section.

4 The Bubble Pump Model

The Equal Velocity Assumption

Lower density material rising in a fluid gives rise to a plume. Such plumes are well described by three equations describing conservation of mass, conservation of momentum and conservation of buoyancy, viz:

$$\frac{d}{dz}(\pi b^2 w) = 2\pi b \alpha w \qquad (1)$$

$$\frac{d}{dz}(\pi b^2 w^2 \rho) = \pi b^2 g (\rho_0 - \rho) \qquad (2)$$

$$\frac{d}{dz}[\pi b^2 w(\rho_1 - \rho)] = 2\pi b \alpha w(\rho_1 - \rho_0)\,. \qquad (3)$$

where α is the proportionality constant relating inflow velocity at the edge of the plume to the vertical velocity within the plume, w, and b is the radius to the plume edge. ρ and ρ_0 are the densities inside and outside the plume respectively and ρ_1 is a reference density for the system. (Morton, Taylor and Turner (1956)).

Plumes widen and slow down as they rise due to the entrainment of surrounding fluid as described by (1).

McDougall (1978) considered bubble plumes specifically, using a similar entrainment assumption, viz: that

$$u_e = \alpha w \qquad (4)$$

where u_e is the (horizontal) entrainment velocity and α is called the entrainment constant.

In both cases developments based on the three conservation assumptions have lead to predictions of plume behaviour in close agreement with plumes observed experimentally.

In the present case one of the underlying assumptions, that of conservation of buoyancy, (3), no longer holds. That is because the bubbles are bubbles of steam-foam rather than of air and such bubbles will tend to collapse as they lose heat to the surrounding water so that buoyancy is not conserved in this case. For this reason it is not possible to model such a plume in the manner of Morton et al, or McDougall. Some other assumptions must be made.

The large theoretical yields calculated in the previous section are entirely a consequence of the buoyancy of the steam-foam injected into the water column by the thin pipe. If this steam-foam were to be instantaneously perfectly mixed with the surrounding colder water the foam would immediately collapse and the yield would be negligibly small. In thermodynamic terms there would be a large increase in entropy entailed in the sudden loss of heat brought about by such mixing.

It follows that the best method of preserving the buoyancy of the foam is to inhibit entrainment and the resulting mixing by containing the plume inside a second pipe. This second pipe will be called here the "fat pipe" to distinguish it from the "thin pipe" which brings the superheated water up from the ocean floor. The cross-sectional area of the fat pipe is assumed to be considerably greater than that of the thin pipe. Apart from suppressing entrainment, the fat pipe also serves to create an ascending column of water around the steam-foam emitted by the thin pipe.

The assumption which we now make and which will allow modeling of the ascending plume to proceed, is that *the vertical velocity of the cold water in the fat pipe is equal to the vertical velocity of the ascending steam-foam plume.*

Instead of a free plume, we now have a steam-foam-driven bubble pump similar to the bubble pumps used in motor-less refrigerator systems but on a much larger scale. Because the relative velocity of the plume and the surrounding water column is zero there will be no entrainment of cold water into the plume in the manner described by (1) and (4) above. If w is zero then so must be u_e.

Fourier's Equation

The single most critical factor determining the viability of such a bubble pump is the lifetime of the steam-foam plume after it comes into contact with cold water.

Inside the foam bubble the conductivity is effectively infinite because liquid is in equilibrium with its own vapour at a fixed pressure. This is the same situation that occurs in a heat pump. If heat is introduced into any part of the mixture the pressure will increase throughout the bubble or vessel so causing condensation and latent heat release elsewhere in the vessel. Because of this heat is transferred extremely rapidly; the rate of heat transfer is dependent only on the speed of sound in the liquid-vapour mixture.

Outside the boundary of the bubble, heat is conducted according to Fourier's equation:

$$\frac{dQ}{dt} = -kA\frac{dT}{dx} \qquad (5)$$

where dQ/dt is the rate of heat transfer, k is the conductivity of the material, A is the cross-sectional area through which the heat is being conducted and dT/dx is the temperature gradient. Equation (5) may be written more succinctly as

$$\frac{\partial T}{\partial t} = \kappa \nabla^2 T \qquad (6)$$

where κ is the ratio of the conductivity to the specific heat of the material and is called the "thermal diffusivity". The Laplacian operator, ∇^2, (pronounced "del squared") is given by

$$\nabla^2 = \frac{\partial^2}{\partial x^2} + \frac{\partial^2}{\partial y^2} + \frac{\partial^2}{\partial z^2} \qquad (7)$$

in Cartesian coordinates.

The thermal diffusivity of water is very small, $\kappa = k/\rho c = 1.456x10^{-7}$ (W/m.K) so that heat diffuses very slowly through water in the absence of convection.

In order to gain an insight into what happens at the boundary between steam-foam and cold water, a simple one dimensional numerical model was set up as depicted in Figure 4.1.

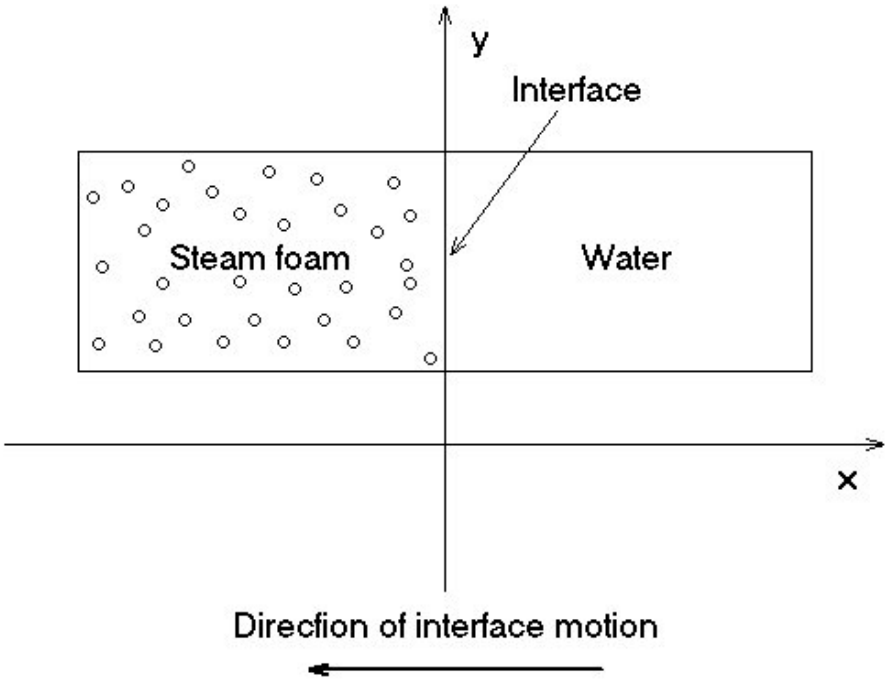

Figure 4.1

In Figure 4.1 steam-foam and water meet at an interface. The interface moves to the left as the steam condenses. The coordinate system moves to the left at the same speed so that the interface always lies at the $x = 0$ plane. In this one dimensional case, (6), becomes

$$\frac{\partial T}{\partial t} = \kappa \frac{\partial^2 T}{\partial x^2} \qquad (8)$$

This parabolic equation is amenable to numerical integration using a " forward time centred space" (FTCS) finite differencing scheme (Press et al 1986), viz.:

$$T_{j,l+1} = T_{j,l} + \alpha(T_{j-1,l} - 2T_{j,l} + T_{j+1,l}) \qquad (9)$$

where $x_j = x_0 + j\Delta x$ and $t_l = t_0 + l\Delta t$, Δx and Δt being the grid spacings in space and time. The parameter α is given by $\alpha = \kappa\Delta t / \Delta x^2$.

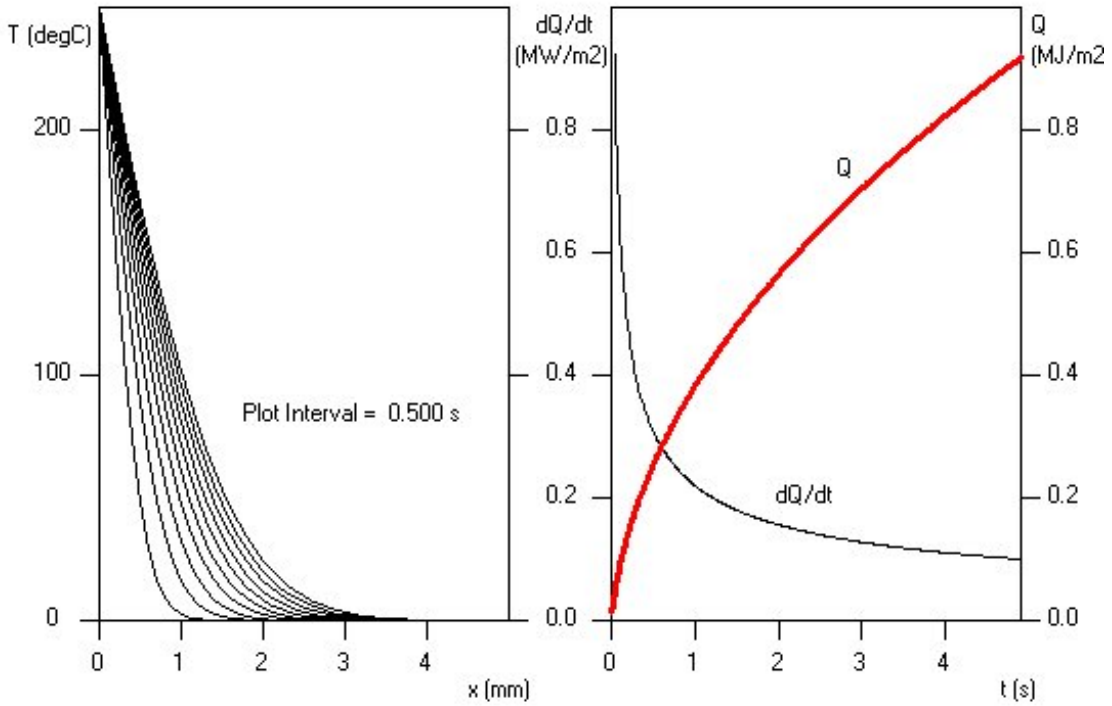

Figure 4.2

The rate of heat transfer across the boundary per unit area per unit time, dQ/dt, was derived from the spatial derivative of the temperature adjacent to the interface, by means of (5), so that

$$\left(dQ/dt\right)_j = \frac{k(T_0 - T_1)}{\Delta x} \qquad (10)$$

The initial conditions were set as

$$T = 250 \text{ for } x \le 0, \text{ and}$$

$$T = 0 \text{ for } x > 0$$

The single boundary condition was

$$T \equiv 250 \text{ for } x \le 0$$

The grid spacings used were

$$\Delta x = .0001 \text{ (m)}$$

$$\Delta t = .01 \text{ (s)}$$

The results for the first 5 seconds of integration are shown in Figure 4.2 The rate of heat transfer fell very rapidly over the first half second or so then leveled out although the cumulative heat transferred per unit area, Q, continued to rise.

More significantly, the heat from the steam-foam only penetrated a short distance into the water. Even after 5 seconds it had barely penetrated 3 mm from the interface.

Rising Spherical Bubble

(i) The Model

The account given above describes an idealized first order model. In order to achieve greater realism a numerical model of a three dimensional "bubble" of steam-foam was constructed. By "bubble" is meant a bubble of steam and water foam such as that emitted by the thin pipe, not the tiny bubbles of pure steam which make up the foam itself. It was assumed that the bubble is rising at the same rate as the surrounding water and is held by surface tension in the form of a sphere which is sufficiently small for the vertical pressure gradient across the sphere to be ignored.

From the time of its creation the bubble not only loses heat to its surroundings but is also expanding due to the pressure drop as it rises through the water column. As it rises it will also cool and this pressure-drop cooling and heat losses due to conduction must be modeled simultaneously. Likewise expansion due to pressure-drop and contraction due to heat loss must also be accounted for simultaneously.

The expansion or contraction of the bubble means that a conventional Eulerian model, in which matter and heat are transported between cells defined by fixed spatial coordinates, is not viable because the most important boundary condition, the location of the surface of the bubble would move relative to these fixed cells. For this reason a Lagrangian differencing scheme was set up whereby boundaries between cells are fixed relative to the moving material, i.e. there is no movement of fluid between cell boundaries which themselves move to accommodate the changing radius of the bubble.

A scheme for numerically integrating Fourier's Equation for the case of a spherical bubble is illustrated in Figure 4.3.

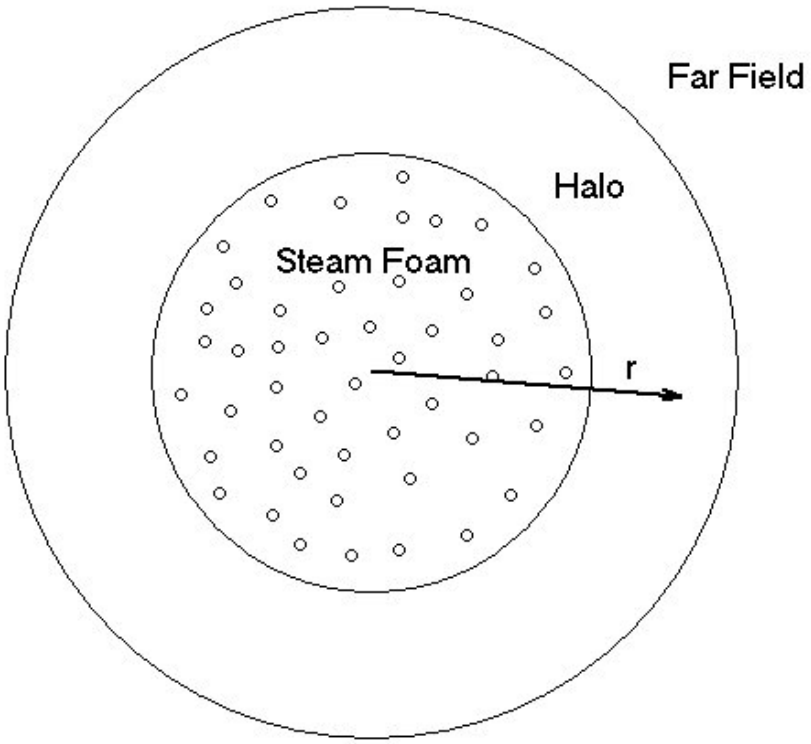

Figure 4.3

In Figure 4.3 a spherical bubble of steam-foam is surrounded by a spherical shell of water heated by the bubble called the "halo". As before we assume that the conductivity inside the bubble is infinitely large. It is the rate at which heat moves through the halo which is the substance of the investigation. For computing reasons it is not desirable that the halo be infinitely large; there is some practical outer radius beyond which heat transfer is irrelevant. This region is termed "the far field".

The halo itself is partitioned into a large number of concentric shells which are the cells of the numerical model. In this spherical coordinate system, the Laplacian operator of (7) becomes

$$\nabla^2 = \frac{1}{r^2}\frac{\partial}{\partial r}\left(r^2\frac{\partial}{\partial r}\right)+\frac{1}{r^2\sin\theta}\frac{\partial}{\partial\theta}\left(\sin\theta\frac{\partial}{\partial\theta}\right)+\frac{1}{r^2\sin^2\theta}\frac{\partial^2}{\partial\phi^2} \qquad (11)$$

We assume spherical symmetry so that all terms containing $\frac{\partial}{\partial\theta}$ and $\frac{\partial}{\partial\phi}$ drop out of the right hand side of (11). After some manipulation (6) becomes

$$\frac{\partial T}{\partial t} = \frac{\kappa}{r}\frac{\partial^2}{\partial r^2}(rT) \qquad (12)$$

where T is the temperature and κ is the diffusivity of water.

An FTCS finite differencing scheme was set up to integrate (12). After each time step in the forward integration of (12) the bubble was assumed to have moved upward through the water column from depth z_l to depth z_{l+1} where

$$z_{l+1} = z_l - w\Delta t \qquad (13)$$

where w is the (constant) vertical velocity of the bubble and Δt is the time step. Pressure was determined at each new depth by interpolating the ambient pressure from the WOCE data set as described previously. From the new pressure a new temperature was calculated using the IAPWS formula for the saturation curve as a function of pressure. From the temperature increment $\Delta T = T_{l+1} - T_l$ the incremental loss, due to boiling, of liquid fraction was found from

$$dF_L = \frac{cF_L\Delta T}{\lambda} \qquad (14)$$

where c is the specific heat of water, F_L is the fraction of the foam that is liquid and λ is the latent heat of steam. New values were then found for the liquid fraction of the foam, $F_L = F_L - dF_L$ and the vapour fraction, $F_v = F_v + dF_L$.

The new density of the liquid phase of the foam was calculated using the formula given by McDougall, Jackett, Wright and Feistel (2002), and the new vapour density of the gaseous phase of the foam was found from the IAPWS formula for saturated vapour density.

The total specific volume of the foam was found by adding the specific volumes of the phases and the density of the mixture, ρ_B, was calculated as the reciprocal of the total specific volume. A new "intermediate" bubble radius, r_B', was then calculated as

$$r_B' = \left(\frac{3m}{4\pi\rho_B}\right)^{1/3} \qquad (15)$$

where m is the mass of the bubble.
The heat loss during the time step, dQ, was found by application of Fourier's Law, (5), to the surface area of the bubble, viz.:

$$dQ = -k(4\pi r'^2)\frac{dT}{dr}dt \qquad (16)$$

The total mass lost by the bubble, Δm, due to this condensation was computed as

$$\Delta m = \frac{dQ}{\lambda} \qquad (17)$$

The new bubble mass, $m = m_0 - \Delta m$, was used to determine a new bubble volume, V, and bubble radius, r:

$$V = \frac{m}{\rho_B} \qquad (18)$$

and

$$r = \left(\frac{3V}{4\pi}\right)^{\frac{1}{3}} \qquad (19)$$

Finally the inner and outer radii for each of the shells in the halo were calculated so that the volume of water in each shell remained constant. Given $a_{j,li}$ and $b_{j,l}$ as the inner and outer radii of the jth shell at time $l\Delta t$, the new radii were found from

$$b_{j,l+1} = \left(b_{j,l}^3 - a_{j,l}^3 + a_{j,l=1}^3\right)^{\frac{1}{3}} \qquad (20)$$

$$a_{j+1,l} = b_{j,l} \qquad (21)$$

$$a_{1,l} = r \qquad (22)$$

These new inner and outer radii were then used in the integration of (12) for the next time step.

(ii) The Initial and Boundary Conditions

The initial conditions for a typical run are shown in Table 4.1. Initial values of bubble temperature was appropriate to a depth of 400m. The vapour fraction was arbitrarily set to 0.3.

Constants

Thermal Conductivity (W/m.degK)	0.600
Specific Heat (J/degK)	4000
Diffusivity (kappa)	.000000146

Dimensions

Minimum Depth (m):	1
Initial Depth (m):	400
Maximum Halo Thickness (m):	0.010

Initial State

Bubble Diameter:	0.300
Bubble Radius:	0.150
Outer Halo Radius:	0.160
Temperature (deg C):	252.270
Halo Temperature (deg C):	9.000
Far Field Temperature (deg C):	9.000
Pressure (dBar):	413.058
Vapour Fraction, Fv:	0.300
Bubble Density (kg/m3):	65.284
Bubble Mass (kg):	0.922924
Total Latent Heat (J):	628511
Vertical Velocity:	10.000

Integration

Time Step, dt (s):	0.100
Radial Step, dr (m):	0.000500
Vertical Step, dz (m):	1.000
Alpha	0.058252
Number of Halo Shells	20

Table 4.1

Two parameters which were varied from run to run were the initial bubble diameter, D_i, and the vertical velocity, w.

The only boundary condition imposed was that the far field temperature was maintained at its initial value.

(iii) Results

Results from a number of model runs are summarized in Figure 4.4

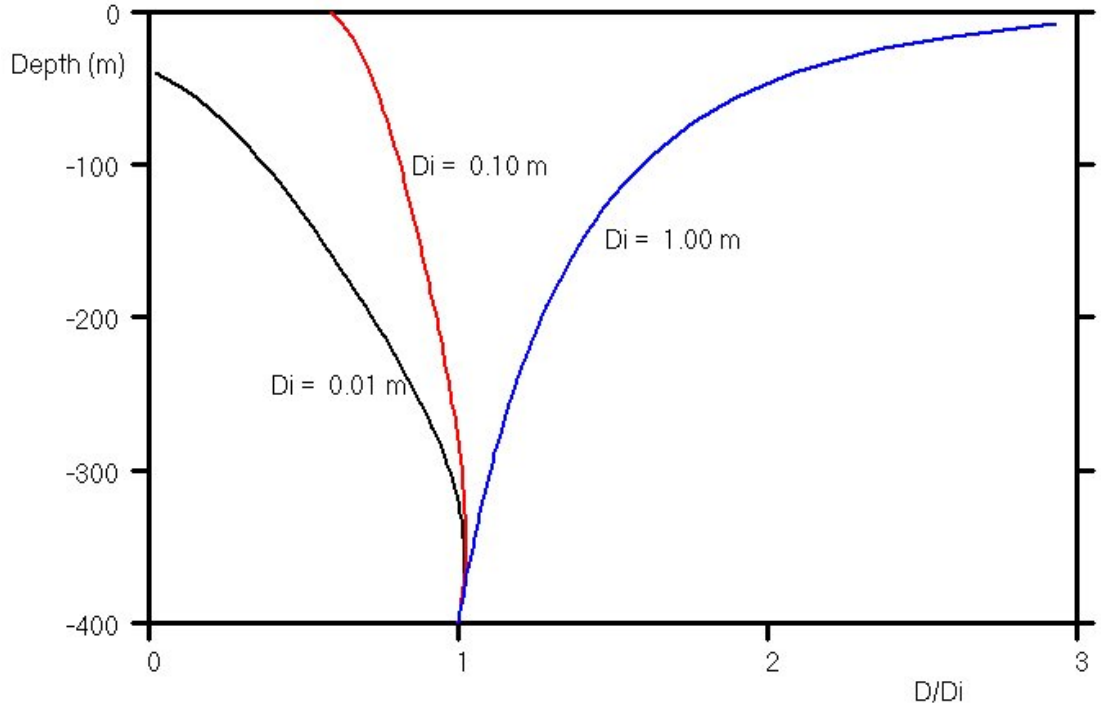

Figure 4.4

Figure 4.4 shows how the bubble diameter changes when the bubble ascends with a vertical velocity of 10 m/s. The ratio of bubble diameter, D, to initial bubble diameter, D_i, is plotted against depth for 3 different values of D_i.
Obviously the diameter and hence the buoyancy of a bubble is a strong function of its initial diameter. Small bubbles lose buoyancy as they rise while large bubbles gain in buoyancy because expansion due to decreasing pressure outweighs contraction due to conductive heat losses. This effect is a direct result of the differing ratio of surface area to volume of different size bubbles.

(iv) Conclusion
Large bubbles behave very differently from small bubbles. The dynamics of steam-foam bubble plumes is strongly dependent on scale.

Steady State Plume

(i) The Model

The previous section described the behaviour of a single isolated bubble of steam-foam surrounded in 3 dimensions by much colder water which extracts energy from the bubble in the form of heat. This is a pessimistic view of the real situation.

In a real steam-foam bubble plume, any single bubble will be accompanied by many similar bubbles all losing heat to their surroundings. In this situation temperature gradients will be much less on average than for a single bubble in isolation.

At this stage we do not know on either experimental or theoretical grounds how a steam-foam plume will break up into individual bubbles although it seems likely that it will do so. One way of dealing with this and so accounting for the proximity of neighbouring bubbles, is to consider a single conical plume of steam-foam rising with the same vertical velocity as the surrounding cold water.

We assume the plume is radially symmetrical rather than spherically symmetrical so that we can use a cylindrical coordinate system rather than spherical coordinate system to describe it. Instead of a rising sphere of steam-foam, we consider a rising disk. The diagram of Figure 4.4 still applies although now it is a section trough a conical plume rather than a section of a sphere.

Another assumption, which may not be justified in practice, is that the rising plume is in a steady state, i.e. that it retains the same three dimensional shape over time.

We follow the behaviour of a disk as it rises through the plume. In cylindrical coordinates (4) becomes

$$\nabla^2 = \frac{1}{r}\frac{\partial}{\partial r}\left(r\frac{\partial}{\partial r}\right) + \frac{1}{r^2}\frac{\partial^2}{\partial \theta^2} + \frac{\partial^2}{\partial z^2} \qquad (23)$$

Radial symmetry implies that $\frac{\partial^2}{\partial \theta^2}$ is zero and we will assume that vertical transport of heat vertically between neighbouring disks is also negligible so that the last term on the right hand side can also be ignored. This gives

$$\frac{\partial T}{\partial t} = \kappa\left(\frac{\partial^2 T}{\partial r^2} + \frac{1}{r}\frac{\partial T}{\partial r}\right) \qquad (24)$$

The finite differencing scheme used for disks was almost identical with that used in the spherical case but with cylindrical expressions replacing spherical expressions. Thus equation (24) replaces equation (12) while equations (13) and (14) remain unaltered. Equation (15) is not used (an intermediate radius is not calculated). Equation (16) is replaced with

$$dQ = -k(2\pi r)dz\frac{dT}{dr}dt \qquad (25)$$

Equations (17) and (18) remain the same and the new radius given by (19) becomes

$$r = \sqrt{\frac{V}{\pi\, dz}}\,. \qquad (26)$$

Top Depth (m):	**0.100**
Injection Depth (m):	**400**
Bottom Depth (m):	**400**
Vertical Velocity (m/s)	**0.500**
Injection Temperature (deg C):	**252**
Halo Temperature (deg C):	**9.000**
Far Field Temperature (deg C):	**9.000**
Injection Pressure (dBar):	**413**
Injection Vapour Fraction:	**0.177**
Injection Volume Flux Rate (m3/s):	**0.075**
Injection Mass Flux Rate (kg/s):	**6.670**
Initial Disk Radius (m):	**0.219**
Time Step, dt (s):	**0.001**
Radial Step, dr (m):	**0.000100**
Vertical Step, dz (m):	**0.001**
Initial Disk Density (kg/m3)	**104.936**
Initial Disk Mass (kg):	**0.007902**
Initial Disk Volume (m3):	**0.000075**
Thermal Conductivity (W/m.degK)	**0.600**
Specific Heat (J/degK)	**4000**
Diffusivity (kappa)	**.000000146**
Alpha	**0.014563**
HaloThickness:	**0.030**
Max Radius:	**0.249**

Table 4.2

Equation (20) becomes

$$b_{j,l+1} = \left(b_{j,l}^2 - a_{j,l}^2 + a_{j,l=1}^2\right)^{\frac{1}{2}} \qquad (27)$$

while (21) and (22) remain unaltered.

As before the new inner and outer radii of the halo cylindrical annuli (rather than shells) were then used in the integration of (24) for the next time step.

An advantage of this steady state plume model was that it was possible during each run to compute the total mass and volume of the plume. Thus the effectiveness of the buoyancy of plume in raising much larger volumes of water up the fat pipe could be computed.

(ii) Initial and Boundary Conditions

The initial conditions for a typical run are shown in Table 4.2. Initial values of bubble temperature, vapour fraction, and density are taken from the output of the thin pipe model for a depth of 400m. The initial halo annular thickness were set to 100 micrometres, but these changed over time as the central steam-foam disk changed it's radius. The initial halo and far field temperatures were set to 9^{o} C, the temperature of the water at the bottom of the fat pipe according to the WOCE data set used.

The sole boundary condition imposed was to maintain the far field at a constant temperature to 9^{o} C.

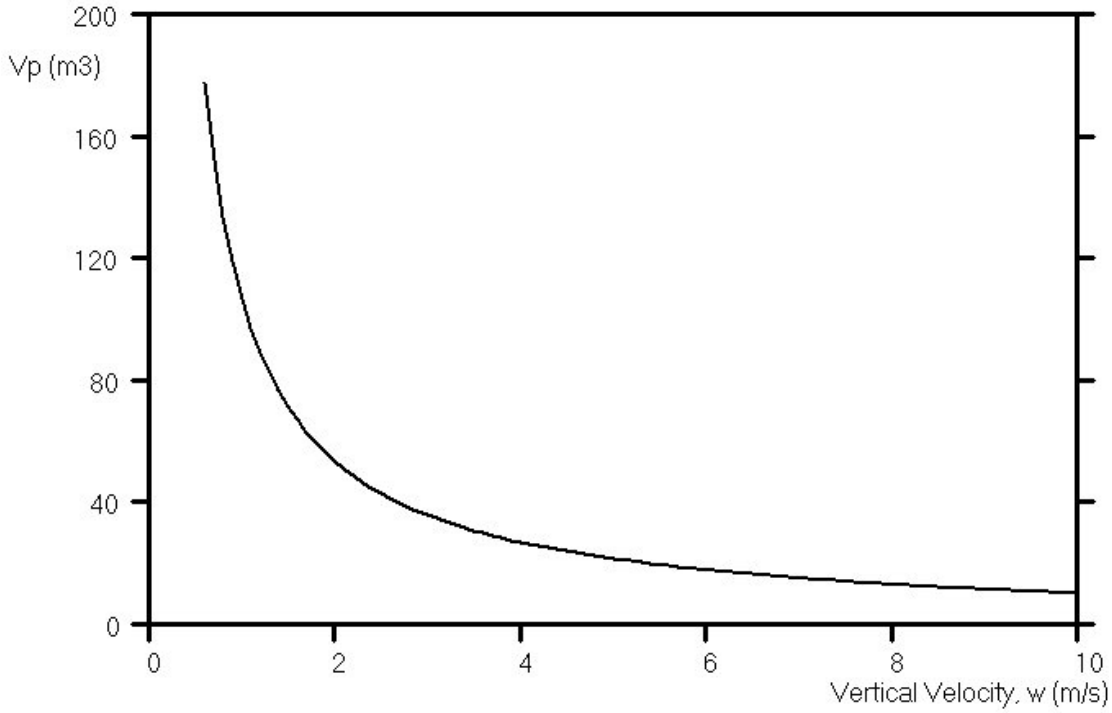

Figure 4.5

(iii) Results

A number of such runs were made in which all initial values were held constant except for the vertical velocity, w, which was varied from 0.5m to 10.0m in 0.1m steps.

Varying the velocity caused large changes in the volume of the plume as can be seen in Figure 4.5. This occurs because as the vertical velocity increase the residence time of each disk of steam-foam in the plume decreases in inverse proportion.

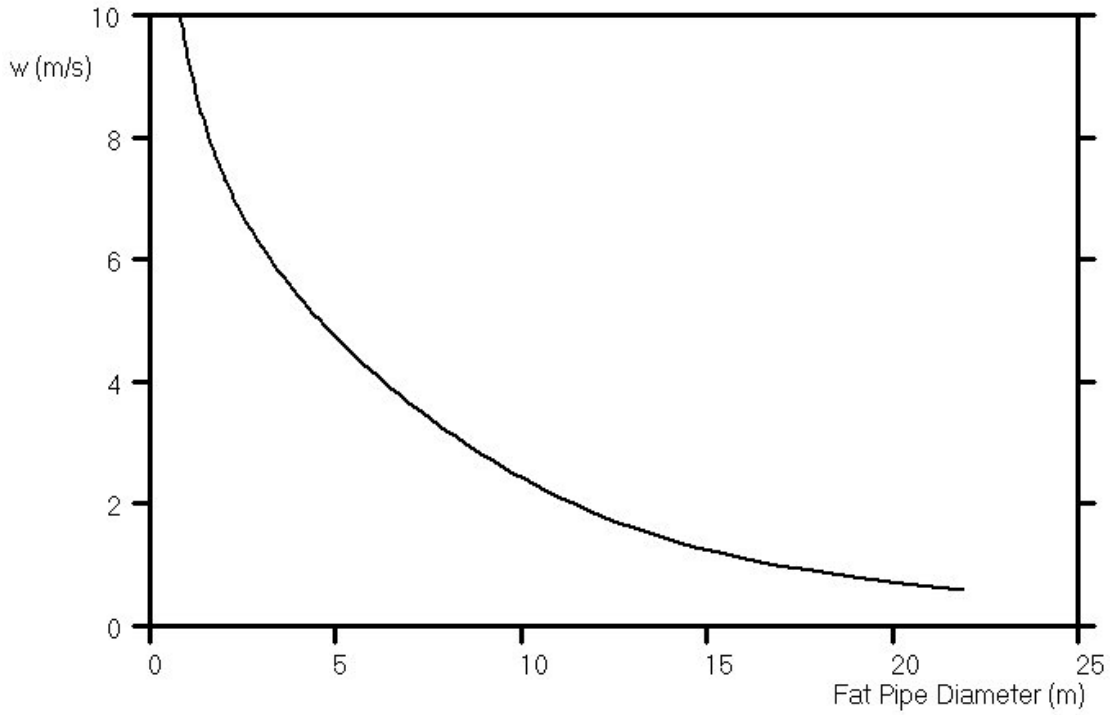

Figure 4.6

Calculating the Fat Pipe Yield

Once the volume and mass of the plume have been found the effective body force on the water in the fat pipe can be calculated. It is convenient to express this quantity as an equivalent head of water, h, i.e. as the difference in water level at the top of the pipe that would create the same gravitational force on the water in the pipe as does the presence of the plume. Expressing the buoyant force in this way allows conventional formulas describing flow in pipes to be used, viz.:

$$h = \phi \frac{L}{D} \frac{w^2}{2g} \qquad (28)$$

Where ϕ is the friction factor, L and D are the length and diameter of the pipe respectively, w is the velocity and g is the acceleration due to gravity.

The head is related to the volume of the fat pipe, V_{fp} , the volume and mass of the plume, V_P and m_P by

$$Ah\rho_{fp} = \left(V_{fp} - V_P\right)\rho_{fp} + m_P - V_{fp}\overline{\rho}_a \qquad (29)$$

where A is the cross sectional area of the fat pipe, ρ_{fp} is the density of water in the fat pipe and $\overline{\rho}_a$ is the density of surrounding seawater averaged over the length of the pipe. Given a vertical velocity, w, the model can be run to determine V_P and m_P from which a head, h, can be determined using (29). From (28) a velocity w' can then be determined.

In general w, and w' will not be the same. However, the fat pipe diameter, D, in (28) was chosen arbitrarily. Providing h is negative (so that w is in the upward direction) it is always possible to iterate to find a suitable value of D which makes the two velocities equal. A plot of fat pipe diameter against vertical velocity is shown in Figure 4.6 with the former plotted as the independent variable.

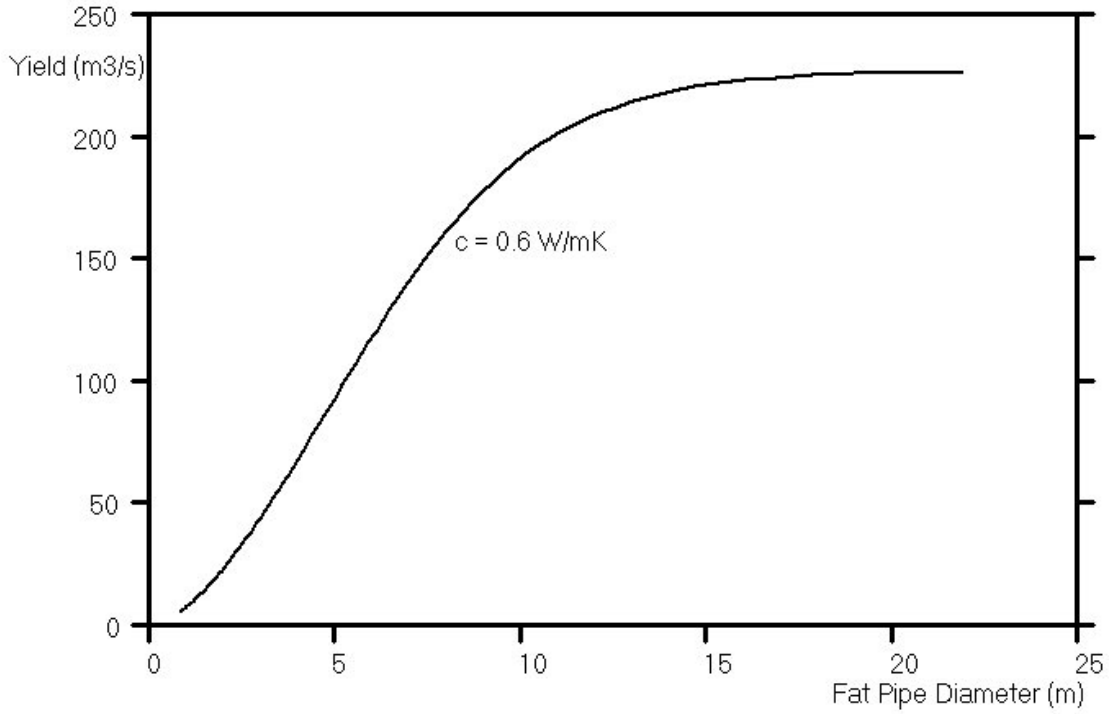

Figure 4.7

Once a vertical velocity has been found in this way the volume flux or yield, Y, of the bubble pump can be determined. Yield as a function of fat pipe diameter is shown in Figure 4.7.

In Figure 4.7 the yield for a 10 MW hydrothermal vent injecting steam-foam into a fat pipe at 400m depth is seen to increase rapidly with fat pipe diameter at small diameters and then to level out to a value of 220 cubic metres per second for larger diameters.

Heat Loss

The heat lost from the rising disk of steam-foam, dQ, was calculated during each time step. This varied considerably as a function of depth. The quantity, dQ, was converted to rate per unit area so as to make it comparable from run to run and plotted against depth. The results are plotted in Figure 4.8.

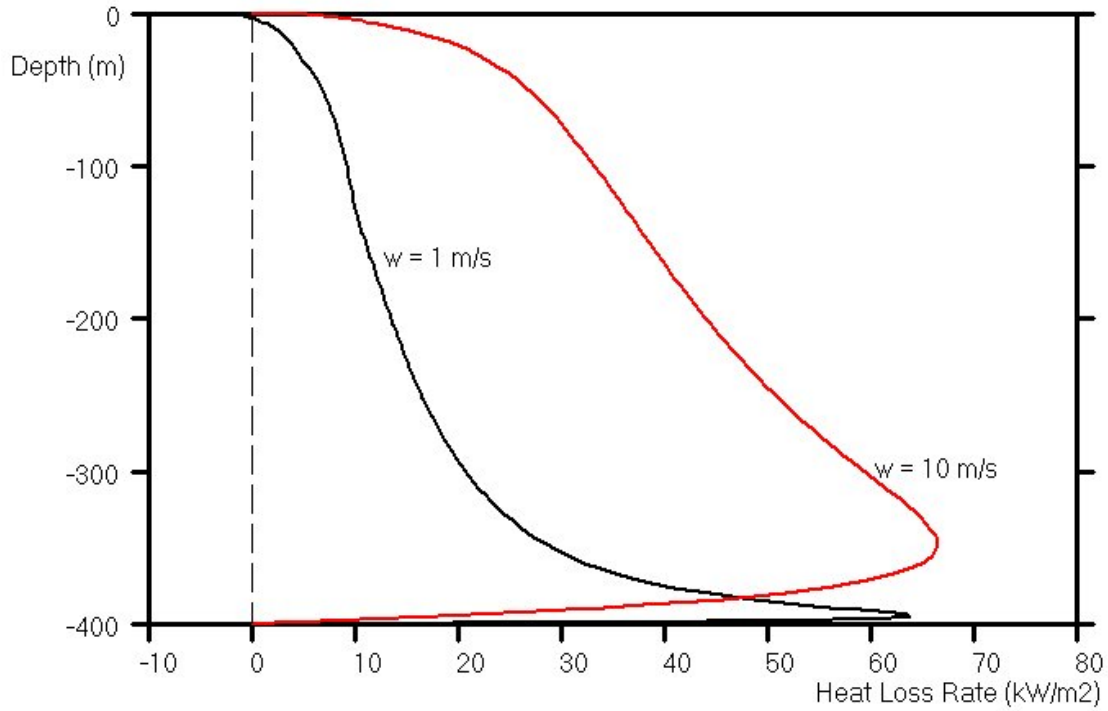

Figure 4.8

As the disk rises there are increasingly large heat losses at first as its surface area gets bigger but then heat loss tails off and even takes small negative values just before reaching the surface.

The heat loss rate becomes negative as the disk approaches the surface. It becomes "self-insulating". Its temperature falls with decreasing pressure according to the saturation characteristic until it finally cools faster due to pressure drop than the halo cools by conduction. Ultimately the disk becomes

cooler than the surrounding halo and heat flows from the halo back into the plume.

Eddy Conductivity

A value of 0.6 W/m.^{o}K listed in Tables 4.1 and 4.2 as the thermal conductivity of water. This is the value of the molecular or "textbook value" of the conductivity. When modeling fluids molecular values for diffusion and conductivity are too small because turbulent eddies on a scale smaller than the grid scale of the model bring about the transport of matter and heat.

This sub-grid-scale eddy transport leads to higher values being adopted known as the eddy diffusion coefficient and the eddy conductivity. These parameters do not have fixed values and depend upon the particular circumstances of each model.

In the present model sub-grid scale turbulence inside the halo region is likely to be small because of proximity to the boundary, however the area of contact between steam-foam and water is likely to be somewhat larger than the value used in the calculations due to instability of the boundary itself. It is impossible to quantify this at this stage but it can be accounted for to some extent by increasing the conductivity to a higher value. The heat transfer rate is linearly dependent on both boundary area and on conductivity so that boundary area increases can be accounted for in this way also.

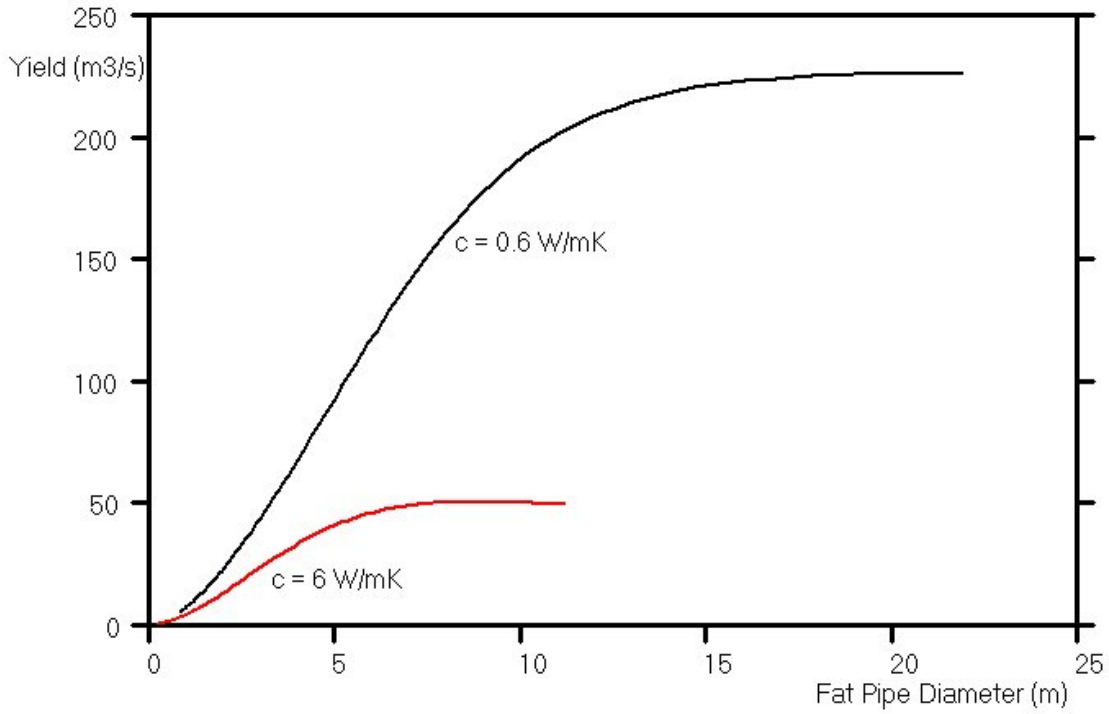

Figure 4.9

The eddy conductivity was increased by a factor of 10, to 6 W/m.^{o}K and the halo thickness increased to 0.1 m to accommodate this higher conductivity value. The effect on yield is illustrated graphically in Figure 4.9. where it is evident that a tenfold increase in conductivity leads to a fivefold reduction in yield.

Thermodynamic Efficiency

Based on potential energy considerations alone the maximum possible yield of a 10 MW HTV injecting at 400m was calculated in the previous section to be 1151 m^3/s. No machine is perfectly efficient. There always losses due to entropy increases incurred by heat losses and friction. The ratio of the actual yield for a heat engine such as this is termed the thermodynamic efficiency.

The thermodynamic efficiency of this hydrothermal bubble pump is estimated according to this numerical model as 20 percent. This compares favorably with the thermodynamic efficiencies of other heat engines such as the steam locomortive (5% to 8%) and the steam turbine (34% to 38%).

Free energy is lost from the system in 3 ways, viz: as heat loss from the foam to the surrounding water, as friction with the pipe walls and in the kinetic energy of the rising water column.

Cold water brought to the surface in this way might be expected to sink back down again immediately after it leaves the fat pipe because it is more dense than the surrounding water. However it also has considerable kinetic energy. The rising water mass will "hit" the ocean surface forcing it to rise a little. The gravitational force on this bulge will dissipate the vertical momentum of the water but leave its kinetic energy unchanged. It will spread out radially beyond the mouth of the fat pipe. It is likely that a toroidal eddy will form.

There will be a considerable velocity gradient between the new water and the surrounding water and entrainment of the surrounding water will occur. As this happens the kinetic energy will cascade down to smaller scales and finish up as turbulent kinetic energy (TKE).

Obviously the situation is not straightforward and further modeling and experimentation is required. Nevertheless it appears likely that the KE of the rising water and the TKE that it generates will cause rapid mixing with the surrounding water and so militate against its sinking back down to the depths whence it came.

Discussion

The lay public and often scientists themselves tend to place too much credence in computer models. The real world must always be more complex than any computer model can encapsulate because real phenomena operate over a large range of scales in a manner that numerical models cannot yet replicate. This means that all numerical models require assumptions, approximations and parameterizations to be made in order for them to be able to work at all. Numerical models are certainly never oracular predictors of real world behaviour. Rather they are heuristic devices which enable us to gain insights into complex physical processes.

The present case is no exception. The underlying "assumption of equal velocity" would certainly not be valid in the real world. The buoyancy of the steam-foam near the centre of the fat pipe must somehow be communicated to the surrounding cold water. There will be a velocity gradient between the upward force of central buoyant fluid and the downward force of the friction in the pipe walls.

Furthermore a rising column of low density fluid such as this will certainly break up into individual bubbles. At present we have no way of knowing how this happens and how small or large these bubbles will be. Figure 4.9 shows a fivefold decrease in yield as a result of a tenfold increase in the area of the steam-foam boundary but this is perhaps a little pessimistic. Ultimately, this issue can only be decided by experiment.

The plume model should be regarded as describing only the gross behaviour of the rising column of steam-foam and of the heat transport therein. The two dimensional heat transfer equation (24) is likely to be a more accurate descriptor of what happens than the three dimensional transfer equation (12) because it takes neighbouring layers into account whereas (12) does not.

Despite these difficulties some important insights have been gained. These include

- Scale size is of fundamental importance,
- Under some circumstances the plume can cool faster than the halo so that the steam-foam becomes "self-insulating",
- Despite free energy losses there is a massive amplification of flow whereby a flow of a few kilograms per second of superheated water is converted to a flow of hundreds of tonnes of cold water. (Seen as a current amplifier, the "gain" is 220,000 / 6.67 or 33,000.) and
- Energy losses in the form of kinetic energy may assist the cold water plume to remain near the surface after it has left the fat pipe.

5 Value of Fishery

Oceanography

The ocean is not the uniform body of water that it may appear to be to the untrained eye. The physical and chemical properties of the ocean vary greatly from place to place in the ocean. Regions of the ocean with similar chemical properties are known as water masses. These water masses mix with one another only very slowly because of their enormous size.

Furthermore water masses are not static but move around inside the ocean. There are two major mechanisms which drive these oceanic flows, viz,:

(i) wind stress (the force exerted by the wind on the surface), and

(ii) thermohaline circulation (density differences due to differences in temperature and salinity).

These deep ocean current flows are measured in units called Sverdrups. One Sverdrup is defined as 1 million cubic metres of water per second moving past a given line. It is a very large unit. The flow of the Amazon is about half a Sverdrup and the combined flow of all the rivers in the world is about one Sverdrup. Continental boundary currents like the East Australian Current are typically about 5 Sverdrup and the biggest flow in the world is between the southern tip of South America and Antarctica and is 500 Sverdrup.

The ocean is also divided vertically. Unlike the deep ocean, the top layer of the ocean is well mixed because of the action of the wind. This is known as the "mixed layer" and its bottom boundary is called the "thermocline". The depth of the thermocline varies from place to place and is the result of a trade-off between the tendency to mix due to wind stress and the tendency to stratify due to solar heating. Generally it is about 50 m deep. The mixed layer roughly coincides with the "euphotic zone", the region in which there is enough light for photosynthesis to take place.

For most parts of the ocean the mixed layer is rather sterile. The blue water in satellite images is blue because very little photosynthesis is happening. There are two notable exceptions to this rule where marine ecosystems bloom, viz.:

(i) Around the margins of continents where river runoff brings nutrients from the land, and

(ii) In regions of the ocean known as "upwellings" where cold nutrient-rich water is brought into the mixed layer by the action of deep ocean currents.

Elsewhere, where there is no such “topping up”, the mixed layer is nutrient-poor because living organisms scavenge it everywhere for nutrients, ultimately export them in the form of corpses, faecal pellets and other detritus which sink below the thermocline. Much of this detritus feeds deep ocean biomass. Some becomes sediment, even deep sediment more or less permanently exported from the atmosphere.

The purpose of this project is to create an artificial upwelling in the belief that this will enrich the ocean by bringing nutrients into the euphotic zone in the same way as natural upwellings.

World fisheries have greatly declined and half of the world’s wild fish depend on natural upwellings occupying 0.1% of world’s ocean surface (WR01, WR02). So we might expect to double the world’s supply of wild fish if we were to triple this flow by adding an extra 0.2% of artificial, HTP upwelling.

Carbon sequestration and Carbon export would also be thus enhanced as discussed in the following section, and these would be of higher quality (for longer durations) than in most other Carbon sequestration systems such as plantations.

The approximate dollar value of man-made nutrient flows can be estimated by placing a dollar value on

(i) Such Carbon sequestration and Carbon export,

(ii) sustained production tonnages of a well-managed pristine, wild fishery based on natural upwellings.

The Namibian Upwelling

The best such example may be the Benguela upwelling off the coast of Namibia. It was one of the last to be exploited, mid-1960s to 1988, and was relatively well managed, and recorded by FAO. The flow of this upwelling is approximately 2 Sverdrups, i.e. 2 million tons of deep ocean water comes to the surface every second (Skogen, 2004) .

Russians and others, mostly Europeans, took approximately 20 million tons of fish out of the Namibian upwelling during the 20 odd year period 1968-88, i.e. at a rate of about 500 kilotons per year per Sverdrup, see "Exploitation, Profile of Catches" (WR04), If this rate exceeded the fisheries' Maximum Sustainable Yield (MSY) it would not have been by very much, because it went on for over 20 years

at a fairly even rate without any catastrophic decline of any catch species' population (WR05).

The Peruvian Upwelling

One of the world's major upwellings occurs off the coast of Peru and supports a major fishery there. This upwelling is about 15 Sverdrups (WR06). This upwelling produced approximately 20 million tons of anchovy per annum during non-El Nino years of which up to 13 million tons pa were taken (WR07 and Idyll, 1973).

Catches of a type of anchovy called anchovetta were above 10 million tons in the late 1960s to 1971 off northern and central Peru. The Peruvian anchovetta population was heavily fished and collapsed during the warming of the 1972 El Niño (WR08). FAO and others worked out an MSY of 10 Megatons per annum for this fishery (WR09 and WR10). Laws (1999) offers a good printed history.

The MSY of the Peru upwelling was thus about 666 kiloton per annum per Sverdrup. This high Peruvian anchovy MSY rate corroborates the 500 kiloton per annum per Sverdrup yield rate for the wider range of species taken from the Namibian upwelling.

These two fisheries were amongst the last fisheries in the world to be exploited and were near-pristine when those measurements were made. They may have been the world's only well studied near-pristine fisheries. They are both "Eastern Boundary Current" upwellings.

Dollar Value of Fishery Based on Natural Upwellings

We propose using overall dollar/ton rates from the most upmarket contemporary fish market, Tsukiji, the wholesale fish market in Tokyo. It moves over 2800 tons of fish per day, i.e. over 780,000 tons of fish per year including over 450 species of fish (WR11). The Tsukiji Fish Market has an annual turnover of more than 2 billion dollars (WR12). In 2007 they sold 780K tons of fish for more than $2 billion implying that the average wholesale price of fish at the world's major fish market is $2600 per ton.

Hence the Namibian catch rate figure of 500,000 tons of fish per year per Sverdrup and the Tokyo average wholesale price of $2600 per ton give a value of $1.3 billion per year per Sverdrup.

Now using the estimated yield of a 10 MW hydrothermal bubble pump of 220 m3/ second, which is 2.2×10^{-4} Sverdrup. Multiplying $\$1.3 \times 10^{9}$ by 2.2×10^{-4} gives $\$2.9 \times 10^{5}$ per year.

Conclusion

The annual return in fisheries product from a single 10 MW hydrothermal bubble pump is estimated to be $290,000.

6 Carbon Sequestration

Will a Plankton Bloom cause Sequestration?

Continuous replenishment of the nutrient in the near-surface layers where sunlight can reach (the euphotic zone) must inevitably lead to a phytoplankton bloom and the depletion of the new nutrient. A good first guess might be that Carbon, Nitrogen and Phosphorus will be consumed according to the Redfield ratio of 108:16:1. However this does not take into account the fact that throughout most of the ocean these three elements are not found in the Redfield ratio. Carbon is invariably greatly in excess of this ratio which reflects the fact that carbon can be dissolved in the ocean by purely physical processes. Thus when a parcel of water is raised to the surface it will contain excess carbon which may be released into the atmosphere over and above that carbon which is taken up by the biota.

The situation is made even more complicated by the complex physical chemistry of CO_2 in water. It reacts with water to form carbonate and bicarbonate ions. Furthermore the reaction rates of the various chemical reactions involved are strong functions of temperature. An excellent description is given by Broecker and Peng, 1982, and will not be repeated here. This complex physical chemistry is encapsulated in the widely-used computer program called CO2SYS of Lewis and Wallace, which allows concentrations and physical parameters to be read in and predictions made of unknown concentrations according to state-of-the-art physical chemistry formulae.

Oceanographic data from WOCE section P18 was input into the CO2SYS program to determine the rate at which carbon would be either sequestered or released when deep nutrients are brought to the surface by means of a hydrothermal heat engine.

Setting the Parameters

Hydrothermal vents occur on mid-oceanic ridges. Their abundance and power are related to the rate of spreading of the plates that define the ridge. For the purposes of this study we take the ridge known as the East Pacific Rise (EPR) as a suitable candidate because it has the fastest spreading rate of any large ocean ridge. Fortuitously, good oceanographic data are available from WOCE (World Ocean Circulation Experiment) section P18 which lies close to the EPR on longitude 105^{o} W and extends from 67^{o} S to 23^{o} N We use this section in this

study. The coloured image at the end of this report shows the distribution of nitrate along this section.

The nitrate density is important because it defines the location and parameters of the hydrothermal pump. The CO2SYS program determines what happens to a parcel of water when it is moved from an input location to an output location. For most of the calculations a depth of 800m at 15° S where nitrate concentration is a maximum was chosen as the input location of the pump and the surface at 15° S was chosen as the output location of the pump.

The various properties of the water parcel were input to the program. These included the salinity, the concentrations of phosphate and silicate, the input temperature and pressure, the output temperature and pressure, the output total alkalinity, TA, and output total carbon, TC. The program then computed the output partial pressure of CO_2, pCO2. The salinity, the concentrations of P and Si and the input temperature were determined by inspection of the relevant WOCE sections.

Input TA and TC and nitrate concentrations were also determined from these sections and the output TA and TC determined from them by assuming that photosynthesis takes place and that this removes carbon and increases alkalinity. The total carbon was assumed to be removed at 6.8 times the nitrate concentration (i.e. according to the Redfield Ratio). Removal of nitrate was assumed to increase the alkalinity by an amount numerically equal to the original nitrate concentration. The computed output TA and TC were also fed to the CO2SYS program to compute the output partial pressure, pCO2.

CO2SYS Predictions

The values discussed above and the computed values of pCO2 are listed in Table 6.1 for a range of output temperatures. The saturation partial pressure of CO2 can be taken as 380 micro-atmospheres corresponding to a concentration in the atmosphere of 380 parts per million by volume as observed by various baseline monitoring stations such as that at Mauna Loa, Hawaii during 2007. The pCO2 values shown in the second last column of Table 6.1 are less than this value for all output temperatures below 27°C, indicating that, in general, carbon will be removed from the atmosphere by the nutrient upwelling, even in tropical latitudes.

In order to arrive at a quantitative estimate of the extent of this carbon removal we need to know the total inorganic carbon concentration which would be achieved if the surface waters were saturated at the specified temperature. This too can be calculated using the CO2SYS program. The values are shown in the third last column of Table 6.1.

The amount of carbon absorbed from the atmosphere can then be calculated by taking the difference between the output total carbon and the saturation value.

These difference values, ΔC, are shown in the final column of Table 6.1. Evidently they are strongly dependent on temperature.

The Effect of Surface Temperature

The effect of variables other than temperature was assessed using the CO2SYS program. Firstly the effect of output depth was tested by taking an output depth value of 50m. The results are shown in the second last row, (b), of Table 6.1. The output values of pCO2 and ΔC are almost indistinguishable from the previously calculated values for a surface output at the same temperature of 25° C.

The values of pCO2 and ΔC were calculated for a temperate latitude (40° S) with different P, Si and nitrate values and lower surface temperature (15° C). The results are shown in the bottom row, (c), of Table 6.1. It can be seen that the computed values (241 micro-atmospheres and 92.5 micromole per kg) are little different from the values at 15° S for the same temperature (233 and 102.7).

				In	In	Out	Out	In	In	In	Out	Out	p=380		
	Sal	P	Si	T	P	T	P	TA	TC	NO3	TA	TC	TC	pCO2	ΔC
	psu	µmol/kg	µmol /kg	°C	dbar	°C	dbar	µmol /kg	µmol /kg	µmol /kg	µmol /kg	µmol /kg	µmol /kg	µatm	µmol /kg
(a)	34.5	3	60	5	800	27	0	2320	2300	43	2363	2008	2004	386	-3.8
	34.5	3	60	5	800	26	0	2320	2300	43	2363	2008	2013	371	5.2
	34.5	3	60	5	800	25	0	2320	2300	43	2363	2008	2022	357	14.1
	34.5	3	60	5	800	24	0	2320	2300	43	2363	2008	2031	343	23.0
	34.5	3	60	5	800	23	0	2320	2300	43	2363	2008	2039	329	31.9
	34.5	3	60	5	800	22	0	2320	2300	43	2363	2008	2048	316	40.9
	34.5	3	60	5	800	21	0	2320	2300	43	2363	2008	2057	303	49.8
	34.5	3	60	5	800	20	0	2320	2300	43	2363	2008	2066	290	58.7
	34.5	3	60	5	800	15	0	2320	2300	43	2363	2008	2110	233	102.7
	34.5	3	60	5	800	10	0	2320	2300	43	2363	2008	2153	184	145.7
(b)	34.5	3	60	5	800	25	50	2320	2300	43	2363	2008	2022	357	14.2
(c)	34.3	2.2	30	4.1	1000	15	0	2295	2200	31	2326	1989	2082	241	92.5

Table 6.1. Data values input to the CO2SYS program. Output values are shown in the last two columns. (a) 800m depth to surface at 15 deg S. (b) 800m depth to 50m depth at 15 deg S. (c)1000m to surface at 40 deg S.

Obviously the major factor controlling the degree of carbon uptake is the final temperature. Water brought up from depth by the hydrothermal pump will always have a much lower temperature than the surface water with which it is mixed and this will bring about some cooling of the final mixture. How much

cooling is problematic because it depends on the degree of mixing and the subsequent heating effect due to solar insolation. The modeling of the output plume from the hydrothermal pump and of the nearby mixed layer promises to be difficult to impossible. All that can be said at this stage is that the carbon sequestration figures listed in Table 6.1 are pessimistic. Because of the cooling effect of the deeper water, more atmospheric carbon will be sequestered than has been calculated here.

Dollar Yield

The ΔC values listed in Table 6.1 enable an estimate to be made of the total rate of carbon sequestered by a single, typical hydrothermal pump.

A spread sheet showing the dollar yield derived from three ΔC values corresponding to three output temperatures is shown in Table 6.2. The carbon credit trading price of $20 per tonne has not been fixed at the time of writing this report. The figure of $20 is little more than a guess.

Conclusion

The phytoplankton bloom generated by a hydrothermal pump will bring about the sequestration of atmospheric carbon even in tropical locations. The rate of sequestration is a strong function of temperature but significant income from carbon trading is possible.

	25 deg C	**20 degC**	**15 degC**	**unit**
HTBP Yield	220000	220000	220000	kg/s
C rate	14.1	58.7	102.7	umol/kg
mol/umol	1000000	1000000	1000000	
C Yield	3.102	12.914	22.594	mol/s
C Atomic Weight	12	12	12	
C Mass Yield	37.224	154.968	271.128	gm/s
kg/g	0.001	0.001	0.001	
C Mass Yield	0.037224	0.154968	0.271128	kg/s
s/day	86400	86400	86400	
C Mass Yield	3216.1536	13389.2352	23425.4592	kg/day
day/year	365	365	365	
C Mass Yield	1173896	4887071	8550293	kg/year
tonne/kg	0.001	0.001	0.001	
C Mass Yield	1174	4887	8550	tonne/year
C Credit Price ($A)	$20	$20	$20	
Dollar Yield	$23478	$97741	$171006	$A/year

Table 6.2. Spreadsheet showing carbon credit dollar yields using 3 values of ΔC from Table 6.1

7 Costing and Deployment Strategies

Component costs are not likely to be excessive. The thin pipe would be made from spoolable insulated pipe which is widely used in the offshore oil industry. It is readily available from a number of manufacturers, e.g. WDS Flexible Pipe (Germany), Aspen Aerogels(US). Either the ocean floor would be drilled and plugged or a funnel shaped cowling could be used to cover an existing HTV.

The fat pipe is fully submerged and is subject to only small lateral pressure differences and can therefore be made from a light flexible material such as polypropylene. A buoyant collar would be required at the upper end. A heavier metal collar may be needed to stabilize the lower end and to provide anchor points for incoming thin pipe. Mooring lines and anchors would also form part of the material costs.

In the early stages, prototypes would be fitted with sensors which would be connected via an umbilical to a separately moored buoy which would transmit data via satellite. Instrumentation and telemetry will need to be included in initial costs.

Excluding instrumentation, component costs are expected to be in the low hundreds of thousands of dollars range.

The greatest cost components are likely to lie in exploration and deployment. Specialist vessels such as those used in the offshore oil and gas industry will need to be chartered for exploration and deployment. Suitable HTVs, indeed whole HTV fields, will need to be identified, mapped and monitored. This will involve keeping such vessels at sea for long periods.

Deployment will require ROVs (Remotely Operated Vehicles) rated for depths of 3000m or so. These too are expensive to charter. In fact new types of specialist ROVs may need to be designed and built for this new technology.

Because these upfront costs are so high compared with component costs it will prove to be more economical to deploy a number of HTBPs rather than a single one in any expedition. A number of thin pipes, each one servicing its own HTV, can be brought together and fed into a single fat pipe.

There is another good reason for doing this: there are "economies of scale" relating to the physics - as the plume gets bigger, energy losses due to heat loss and foam collapse are proportionally smaller, as suggested in Section 4.

Deploying a number of HTBPs distributed contiguously over a region of ocean has three further advantages:

1. Their individual nutrient plumes will merge into a single large plume, and
2. A larger area plume will tend to be more confined by coriolis force into a single large eddy. This has advantages from a fisheries management perspective and these first two benefits imply that

3. A large array of HTBPs may not require any fat pipe.

At the time of writing it was too early for any detailed costing to be carried out. The offshore oil and gas industry has extensive knowledge and expertise in this area, particularly regarding the thin pipe risers and interfacing the thin pipes to the ocean floor. Only the fat pipe technology is really new. This technology is more closely related to fish cage manufacturing techniques.

8 Other Methodologies

Four alternative methods of ocean fertilization are known to the authors, viz.:

1. Oceanographer John Martin disclosed a method for fertilizing High Nutrient Low Chlorophyll (HNLC) areas of the ocean with iron in order to stimulate phytoplankton growth so as to absorb atmospheric CO2 (Martin,1990). The practicality of the method has been convincingly demonstrated experimentally. However the method is limited to HNLC regions of the ocean where there is already a high nitrogen concentration.

2. Another method of artificial ocean mixing would be to use an Ocean Thermal Energy Conversion (OTEC) device to bring deep nutrient rich waters to the surface. Such a device has been in operation in Hawaii for a number of years. The nutrient rich waters are fed into on-shore fish farms.

3. An apparatus for artificial ocean mixing has been proposed whereby a flexible vertical pipe with a valve pumps deeper water to near the surface by wave action. (Kithil and Boeing: Ocean Carbon Biogeochemistry Workshop, Woods Hole Oceanographic Institute, July 10-13,2006). A similar idea has been proposed by James Lovelock.

4. Ian Jones of the University of Sydney has proposed using fixed-nitrogen products such as urea, made on land, to fertilize low nitrogen regions of the ocean.

Of these only the first is likely to prove both economic and viable. There have been a number of experiments that have demonstrated that distributing iron in the ocean does indeed lead to an increased phytoplankton productivity. Whether this leads in turn to greater sequestration of atmospheric CO2 remains in question. Absence of experimental evidence for this is largely the result of the relatively short time scale of oceanographic cruises.

An excellent review of this work has been given by Falkowsky (2002) who points out that some serious difficulties with the method remain. To quote him:

Major disruptions to the marine food web are a foremost concern. Computer simulations and studies of natural phytoplankton blooms indicate that enhancing primary productivity could lead to local problems of severe oxygen depletion. The microbes that consume dead phytoplankton cells as they sink

toward the sea floor sometimes consume oxygen faster than ocean circulation can replenish it. Creatures that cannot escape to more oxygen rich waters will suffocate.

Such conditions also encourage the growth of microbes that produce methane and nitrous oxide, two greenhouse gasses with even greater heat-trapping capacity than CO2.

None of the other three methodologies can deliver the quantity of nutrient required at sufficiently low cost. In order to compare with the 220 m3/s yield of an HTBP calculated in Section 4 an ocean wave device would need to intersect the waves across 4 km of ocean. This is assuming 100 percent efficiency. The fact that, despite several decades of work in this field, no viable offshore wave power device has yet been contrived makes this solution look rather fanciful.

Nevertheless, Method 4, artificial fertilization by means of land based chemicals may provide a useful adjunct to the method proposed here, for fine tuning its artificial marine ecosystem. The major problem with both the iron method and the urea method is that they do not address the issue of phosphorous depletion. Phosphorus is essential in the production of nucleic acids and its absence would provide a major limitation to plankton growth.

9 Side Effects and Consequences

There is no doubt that a radical new technology such as that described here will inevitably have a number of negative consequences. Some of these can be predicted or at least hinted at while others may not become evident until the program is well under way. All we can do here is make the best informed guesses that we can about what some of these may be.

Consequences fall into many different categories, physical, chemical, biological, environmental, legal, political and so on. Discussion under these headings follows.

Physical

Large bubbles of low buoyancy sea foam regularly break the surface above the mouth of the fat pipe. A canoe or small boat could fall into one and sink like a cork in a rapidly boiling saucepan.

The sea foam is boiling so there will always be a plume of steam rising into the sky. This steam plume will smell of bad eggs like hot springs often do, and is likely to trigger water spouts in the right atmospheric conditions. Acid rain will fall out of it, but only over a small region. The steam plumes will become known to navigators as places to steer clear of.

Chemical

The effluent from HTVs contains some nasty chemicals and these are brought almost undiluted to the top end of the thin pipe. They include heavy metal sulphides and hydrogen sulphide and will be rapidly oxidized to sulphurous and sulphuric acid.

Some of the metal sulphides could have commercial value and it may be worth harvesting the precipitates that form inside the fat pipe.

However, once the bubbles break the surface and the foam starts to cool, it will rapidly mix with surrounding water. The "gain" of 33,000 reported at the end of Section 4 is also the dilution factor within the fat pipe. The poisons will be diluted yet again as the turbulent nutrient plume emanating from over the top of the submerged fat pipe mixes with surrounding surface water.

Furthermore, hydrothermal vents have been pumping these chemicals into the sea for billions of years. Life has grown up adapting to them, even needing some of them. They are not poisons like dioxin or plutonium which are alien to living things. They are just common ocean chemicals in higher concentrations than usual. They rapidly become harmless once they are diluted by natural processes.

Biological

Unlike the artificial fertilization schemes discussed in the previous section, the various HTBP nutrients remain in the same proportions overall as they do in the rest of the ocean. They are also much more dilute. Hence the problems associated with iron fertilization simply will not happen.

The upwellings created artificially using HTBPs closely resemble natural upwellings in all but two respects: the vertical velocity is much greater and the nutrient plume is more localized. This may have unintended consequences in the development of the biota bloom, but it is impossible to predict what they will be.

Environmental

Intuitively it seems that mixing the ocean can only be good for life in general, given that the process reverses the well known destructive effect of man's fishing of the world's oceans. Nevertheless there may be short term or localised problems that will need to be considered.

Legal / Political

At first HTBPs will no doubt be deployed in the territorial waters of one or more nation states. Japan comes to mind as a likely HTBP participant; a developed country with capital to invest, a taste for fish and plenty of tectonic activity within its borders. However, the inshore development sites around tectonically active countries like Japan and Indonesia will soon be used up and the industry will need to move further offshore.

In the long term, the best places to deploy HTBPs will be above mid-oceanic ridges which lie, by and large, outside territorial waters, i.e. on the high seas. Jurisdiction is therefore a matter of Law of the Sea which has yet to evolve to deal with issues likely to arise as a consequence of this technology.

A company investing millions of dollars in setting up an artificial fishery with HTBPs on the high seas is unlikely to take kindly to others taking its fish, but under present law there would be no way to prevent this from happening short of taking up arms.

In the interest of good relations between nations, investors will need to be assigned some sort of jurisdiction or else they may take the law into their own hands and employ private navies to guard their investment.

Envisage the Japanese developing a vent field on the East Pacific Rise somewhere south of Easter Island. As the fish stocks become larger and closer to commercial exploitation, Chilean and Peruvian fishing boats appear and start taking fish. What are the Japanese going to do about it? What about large migratory species like tuna or whales that will certainly visit from time to time and eat their fill? Who owns the tuna, the whales?

Another legal matter is the issue of carbon credit trading. Will companies and nation states be able to claim carbon credits for carbon sequestered offshore, on the high sea, or even in some other nation's jurisdiction?

10 Discussion

Back of Envelope Calculations

Here are some "back of envelope" calculations intended to put the ideas presented above into a global perspective.

The calculations in Section 6 on Carbon Sequestration were based on WOCE data for the East Pacific where there is a large amount of nitrate and phosphate present at depth in the ocean. Using WOCE sections P18 and P21 it turns out that the nitrate bearing waters extend 5000 km N-S, 7000 km E-W and have a depth range of 1500m giving the total volume of the nitrate bearing waters of 5 x 10^{16} m^3. The average concentration of nitrate is about 35 µMol / kg which leads to a total mass of nitrate of 114 Pg (1 Pg = 10^{15} g, pronounced "petagram").

For tropical waters at about 21°C, according to Table 6.1 carbon is removed from the atmosphere at about the same molar rate as the nitrate brought up by the HTBP. Hence that East Pacific nitrate mass has the potential to remove about the same amount of CO2 from the atmosphere, i.e. about 100 Pg. The total amount of CO2 in the atmosphere is around 700 Pg which means that the East Pacific nitrate mass has the potential to reduce atmospheric carbon by about 14 percent.

And that is using only one part of one ocean! Using other nitrate masses in other parts of the ocean we could perhaps remove *all* of the atmospheric CO2 and trigger another ice-age.

There is very little likelihood of that happening however. The HTBP brings up 220 m^3/s which is 7.3 X 10^9 m^3/year. Using the total volume calculated above it would take 5 x 10^{16} / 7.3 X 10^9 or about 7 million years for this to happen with a single HTBP. Even with 1000 HTBPs it would still take 7000 years. So there will be plenty of time to study consequences and to take corrective action.

There is really no need to worry about ice-ages as an unintended consequence of deploying HTBPs.

The "Tampering" Argument

One of the most persistent arguments we have heard voiced against our idea is the idea that we are "tampering with Nature". This is not a scientific argument, it is a religious one, but it still requires an answer nonetheless.

In one sense every time someone ploughs a field or undergoes a triple bypass procedure, we are tampering with Nature. Mankind has been tampering with Nature since the invention of agriculture. It is now happening to such a degree that people are genuinely worried about the consequences, so why don't our critics want us to "tamper" Nature back to how it was or how it "should be"?

The answer lies in the intent. Instead of planet-wide effects happening by accident as it were, we *intend* to deliberately change the planet by an effort of human will. This modern sentiment still arouses humanity's deepest fears about "hubris" and confronting the gods as it has in the past. It would remind many of Nietzsche and the Nazis. But history shows that it is societies that overcome these fears and get on with it who will ultimately be the most successful biologically. The rest will remain trapped by their superstitions.

It has always been this way when any new machine has come along; when there is a quantum leap in technology rather than a steady evolution. These fears are soon forgotten as people get used to the new machines and practices and find that their benefits outweigh their shortcomings. We no longer require motor vehicles to be preceded by a man displaying a red flag.

Furthermore the construction and deployment of HTBPs is not a sudden process. As more and more of them come online scientists will be watching for environmental impacts, not because of some law that requires an EIS to be carried out but because the effectiveness of the HTBP as a money earner will be at stake. As problems crop up they will be fixed just as they were in every other new technology. This will be a boon for oceanographers and marine biologists.

Hunter-Gatherers and Farmers

If this project is successful, and HTBPs start to be deployed in ever larger numbers, it will represent a sociological shift similar to the invention of agriculture. As it stands now, fishing is still an activity of hunter-gatherers. Only nowadays the hunters have GPS and depth sounders and vessels that stay at sea for a year at a time with nets as big as skyscrapers. There is huge**,** destructive competition for the resource. It is a classic example of Gareth Hardin's "The Tragedy of the Commons". Despite all the fisheries regulations and all the pious international committees, the rape of the oceans still goes on.

Introducing HTBPs into this scenario revolutionizes it and makes fishing the oceans much more like farming. There will be an investment to look after. Over-fishing becomes foolish not merely unfortunate because it depreciates the value of the investment. The legal and political issues discussed in the previous section can and must be overcome.

Using geothermal energy to mix the ocean offers the potential for the ocean to become the new prairie, the new steppe.

.

11 Acknowledgements

The author is indebted to Dr Trevor McDougall and David Jackett of the Division of Marine and Atmospheric Research of CSIRO without whose advice this idea may never have come into existence. The author would also like to thank Dr Simon Wright of the Australian Antarctic Division, Professor Tom Trull of the Institute of Antarctic and Southern Ocean Studies, Dr John Parslow of the Division of Marine and Atmospheric Research of CSIRO and Alex Papij of Turo Technologies Pty Ltd, for their helpful advice and comment.

References

Literature References

Broecker,W.S. and T-H Peng. (1982) "Tracers in the Sea". Lamont-Doherty Geological Observatory.

Falkowsky, P.E. "The Ocean's Invisible Forest". *Scientific American*, August 2002.

Idyll, C. P. (1973) *Sci. Amer.* **228**(6), 22

Laws, E. A. (1999).“El Niño and the Peruvian Anchovy Fishery”. Edited by Edward A. Laws, Journal Reviews in Fish Biology and Fisheries, Springer Netherlands, ISSN 0960-3166 (Print) 1573-5184 (Online), **9**, 1 pp118-121.

Lewis, E., and D. W. R. Wallace. (1998). Program Developed for CO2 System Calculations. ORNL/CDIAC-105. Carbon Dioxide Information Analysis Center, Oak Ridge National Laboratory, U.S. Department of Energy, Oak Ridge, Tennessee. (http://cdiac.ornl.gov/oceans/co2rprt.html).

Martin J.H. (1990). "Glacial-interglacial CO2 change: The iron hypothesis." *Paleoceanography* **5(1)**: pp 1-13.

Morton, B.R.,G. Taylor and J. S. Turner. (1956). "Turbulent gravitational convection from maintained and instantaneous sources". *Proc. Royal Soc. A,* **234**, pp1-23.

McDougall, T.J. (1978). "Bubble plumes in stratified environments". *J. Fluid Mech.* **85**, **part 4**, pp655-672.

McDougall, T.J., D R. Jackett, D.G. Wright, and R. Feis. (2003) “Accurate and Computationally Efficient Algorithms for Potential Temperature and Density of Seawater”. *J.Atm. Ocean Technology*, **20**, 5.

Skogen, M.D. (2004); “A direct estimate of the Namibian upwelling flux.” Accepted for publication in: Ecological, economical and social aspects of Namibian fisheries. U. R. Sumaila, S. I. Steinshamn, M D. Skogen and D. Boyer (eds), Eburon Publishers, Delft.

Wagner, W and H-J Kretschmar (2007) “International Steam Tables: The Industrial Standard IAPWS-IF97 for the Thermodynamic Properties and

Supplemetary Equations for Other Properties: Tables, Algorithms, Diagrams, Software", Springer.

Web References

WR01
http://news.bbc.co.uk/2/hi/science/nature/6108414.stm

WR02
http://www.abc.net.au/rn/scienceshow/stories/2007/2119482.htm

WR03
www.imr.no/__data/page/5133/A_direct_estimate_of_the_Namibian_upwelling_flux.pdf

WR04
http://firms.fao.org/figis/website/FIRMSRetrieveAction.do?dom=resource&fid=13330

WR05
http://firms.fao.org/figis/common/format/popUpImage.jsp?xp_imageid=1697

WR06
see Peru Current entry at:
http://stommel.tamu.edu/~baum/paleo/ocean/node30.html

WR07
http://www.fao.org/docrep/005/y2787e/y2787e0b.htm

WR08
http://www.pfeg.noaa.gov/research/climatemarine/cmffish/cmffishery4.html

WR09
page 54 at
http://books.google.com/books?id=kfv059OL6kQC&pg=PA54&lpg=PA54&dq=fao+10+million+tons+peruvian+upwelling&source=web&ots=J2v9Kz1f7F&sig=RyhDA7Z9szf8mBLyt3Wc2758JM0

WR10
page 44 at
http://books.google.com/books?id=FZvLx3x9tYsC&pg=PA44&lpg=PA44&dq=msy+peruvian+upwelling&source=web&ots=FqaRC21Qfy&sig=G-4v7Uz90sok3vFWsYP2RA53xz0

WR11
www.links.net/vita/trip/japan/food/tsukiji/

WR12
www.marunaka-net.co.jp/maruna_e/aisatu.htm

WDS Flexible Pipe
http://www.porextherm.de/images/daten/doc_63_en.pdf

The World Ocean Circulation Experiment (WOCE)
WOCE data for the Pacific Ocean can be found at
http://www-pord.ucsd.edu/whp_atlas/pacific/p18/sections/sct_menu.htm